A Catchment-Scale Hydro-Biogeochemical Model for Studying Non-Point Source Nitrate transport and Denitrification Process

Yipei Wen[1], Jeen-Shang Lin[1], Fernando Plaza[1], and Xu Liang[2]

[1]University of Pittsburgh
[2]University of Pittsburgh, Pittsburgh

November 28, 2022

Abstract

Rainfall runoff and leaching are the main driving forces that nitrogen, an important non-point source (NPS) pollutant, enters streams, lakes and groundwater. Hydrological processes thus play a pivotal role in NPS pollutant transport. However, existing environmental models often use oversimplified hydrological components and do not properly account for overland flow process. To better track the pollutant transport at a watershed scale, a new model is presented by integrating nitrogen-related processes into a comprehensive hydrological model, the Distributed Hydrology Soil and Vegetation Model (DHSVM). This new model, called DHSVM-N, features a nitrate transport process at a fine resolution, incorporates landscape connectivity, and enables proper investigations of the interactions between hydrological and biogeochemical processes. Results from the new model are compared with those based on Soil & Water Assessment Tool (SWAT). The new model is shown capable of capturing the "hot spots" and spatial distribution patterns of denitrification, reflecting the important role in which heterogeneity of the watershed characteristics plays. In addition, a set of control experiments are designed using DHSVM-N and its variant to study the respective role of hydrology and nitrate transport process in modeling the denitrification process. Our results highlight the importance of adequately representing hydrological processes in modeling denitrification. Results also manifest the importance of having a good transport model with accurate flow pathways that considers realistic landscape connectivity and topology in identifying the denitrification hot spots and in properly estimating the amount of nitrate removed by denitrification.

A Catchment-Scale Hydro-Biogeochemical Model for Studying Non-Point Source Nitrate transport and Denitrification Process

Y. Wen[1], J-S. Lin[1], F. Plaza[1], and X. Liang[1*]

[1]Department of Civil and Environmental Engineering, University of Pittsburgh, Pittsburgh, Pennsylvania, USA.

*Corresponding author: Xu Liang (xuliang@pitt.edu)

Key Points:

- A new hydro-biogeochemical model, DHSVM-N, is presented that gives reasonable spatial denitrification patterns from nitrate transport.
- Landscape unit connectivity, routing and flow paths are critical components in transport for simulating hot spots of denitrification.
- The physically based model presented is capable of providing source-to-endpoint pathways of nitrate transport.

Abstract

Rainfall runoff and leaching are the main driving forces that nitrogen, an important non-point source (NPS) pollutant, enters streams, lakes and groundwater. Hydrological processes thus play a pivotal role in NPS pollutant transport. However, existing environmental models often use oversimplified hydrological components and do not properly account for overland flow process. To better track the pollutant transport at a watershed scale, a new model is presented by integrating nitrogen-related processes into a comprehensive hydrological model, the Distributed Hydrology Soil and Vegetation Model (DHSVM). This new model, called DHSVM-N, features a nitrate transport process at a fine resolution, incorporates landscape connectivity, and enables proper investigations of the interactions between hydrological and biogeochemical processes. Results from the new model are compared with those based on Soil & Water Assessment Tool (SWAT). The new model is shown capable of capturing the "hot spots" and spatial distribution patterns of denitrification, reflecting the important role in which heterogeneity of the watershed characteristics plays. In addition, a set of control experiments are designed using DHSVM-N and its variant to study the respective role of hydrology and nitrate transport process in modeling the denitrification process. Our results highlight the importance of adequately representing hydrological processes in modeling denitrification. Results also manifest the importance of having a good transport model with accurate flow pathways that considers realistic landscape connectivity and topology in identifying the denitrification hot spots and in properly estimating the amount of nitrate removed by denitrification.

Plain Language Summary

Existing hydro-environmental models for nitrogen pollution assessment often focus on stream water quality and their simplified hydrological considerations may be acceptable for this narrow focus, but not when its spatial patterns within a watershed are important which are influenced by comprehensive hydrological processes and the flow paths nitrogen takes to reach stream channels. To study nitrogen-related process and the associated nitrogen patterns overland, it is important to consider hydrological processes adequately together with the flow pathways which are governed by topography. In this context, a new model, DHSVM-N, which incorporates comprehensive and detailed hydrological processes, is developed. By modeling nitrate transport processes at a fine spatial resolution using realistic landscape connectivity, the new model can properly account for interactions between hydrological and biogeochemical processes. The new model shows great potential in modeling denitrification, a key natural reactive nitrogen removal process, and is able to adequately capture its spatial patterns within the watershed domain. DHSVM-N is further used in investigating factors that are crucial in modeling denitrification. In comparison with existing models like SWAT, we have shown the important role of hydrological processes and nitrogen transport model played in simulating hot spots as well as the total amount of denitrification.

1 Introduction

Agricultural pollution, usually associated with excessive use of fertilizer and other agricultural activities, is a major source of nonpoint source (NPS) pollution. NPS pollutants, reaching rivers and lakes via rainfall runoff and leaching, cause deterioration of water quality and threaten public health and biodiversity. NPS pollution has been identified as a major factor of water impairment by the United States Environmental Protection Agency(EPA, 2002). Agriculture-source nitrogen pollution is a common type of NPS pollution. The large amount of fertilizers used in combination with irrigation process is reported as a main reason causing increased nitrate concentration in both surface water bodies and groundwater system in agricultural watersheds (Torres-Martínez et al., 2021). For instance, it has been estimated that up to 81% of total water pollution in China is contributed by NPS nitrogen pollution (Ongley, Xiaolan, & Tao, 2010). In Europe (EEA, 2007) this type of pollution is also reported as the cause of environmental issues like eutrophication, whereas in Gulf of Mexico, hypoxic zone has been found expanding with ever increased negative impacts on both environment and economy (Sinha, Michalak, & Balaji, 2017).

Modeling NPS nitrogen pollution is quite challenging because of the complex nature of the problem. However, modeling is an indispensable part of an assessment effort and sometimes even a preferred one for if it is done right, it could provide invaluable insights in discerning various scenarios and reaches objective assessments of impacts of pollution and effectiveness of mitigation measures. There are a number of hydro-environmental models currently being applied for estimating NPS nitrogen pollution. Among them, the most widely used one is Soil & Water Assessment Tool (SWAT), other popular ones include Integrated Catchment Model (INCA), Agricultural Non-Point Source Pollution Model (AGNPS/AnnAGNPS), Hydrological Simulation Program - Fortran (HSPF) and Hydrologiska Byråns Vattenbalansavdelning Model (HBV) (Wellen, Kamran-Disfani, & Arhonditsis, 2015). Problems remain, however, because behind the development of many environmental hydrological models, there is a lack of communication and common language between catchment-hydrology and water quality communities (Hrachowitz et al., 2016). Uncertainties also arise as models are often applied in ways for which they are not originally developed (Wellen et al., 2015).

Followings are three major limitations of current environmental-hydrological models: The first major limitation stems from the oversimplified representation of landscape topology, namely the spatial modeling units are not connected for the water and solute transport processes. Transport models they adopted may very well be robust, but the critical movement of water and pollutant that are required to represent detailed biogeochemical processes (Hrachowitz et al., 2016) often are simplified to such extent that upland areas are connected directly to downstream channels without flowing over land. This is a serious issue if impacts of overland pollutant are at stake. In addition, by not having overland flow their pollutant transport processes ignore interactions between pollutants and their ambient environment along the transport flow paths (Shen, Liao, Hong, & Gong, 2012), even though some amend it by adopting “black box” like empirical approach controlled by tunable parameters. Lacking flow paths between source and sink areas undermines these models’ ability to properly identify “hot spots” of the biogeochemical processes (Mitchell, 2001; Wellen et al., 2015), and the lack of interactions among the spatial units in these models has been recognized as a crucial weakness (Arnold, Allen, Volk, Williams, & Bosch, 2010; Bosch, Arnold, Volk, & Allen, 2010; Gassman, Reyes, Green, & Arnold, 2007).

The second major limitation results from oversimplified hydrological processes. For example, SWAT adopts the curve number (CN) method for computing runoff, but this empirical method assumes infiltration-excess runoff and has problems of adequately identifying runoff prone areas if saturation excess runoff is the dominant runoff generation mechanism. Studies have also shown that SWAT is inadequate in modeling hydrology and pollutant export for areas controlled by variable source area (VSA) hydrology, where most of the surface runoff is generated by relatively small contractable areas via saturation excess runoff (Easton et al., 2008; Hoang, Schneiderman, et al., 2017; White et al., 2011; Woodbury, Shoemaker, Easton, & Cowan, 2014). SWAT is often calibrated against streamflow observations at a watershed outlet and thus good streamflow results could be obtained at the outlet, but they are obtained at the expense of unrealistic watershed internal processes. This is not uncommon for a high degrees of freedom complex system that reasonable results could be obtained with physically unrealistic parameters when the observational data for calibration are limited (Beven, 2006). For example, high CN number would be assigned in SAWT to compensate its inability in correctly representing surface runoff contribution from runoff-prone areas within a watershed; more water, as a result, is partitioned to surface runoff than to soil moisture, and the spatial distribution of the soil moisture within the watershed is misrepresented. This could lead to serious problems in studying biogeochemical processes within the watershed as soil moisture is a critical factor. In other words, a model's successes, such as by SWAT, in matching streamflow at the watershed outlet with observations could have all these drawbacks wrapped underneath.

Combination of the above two shortcomings lead to the third limitation: heterogeneous biogeochemical processes like denitrification, which are key factors needed in many best management practices decisions, could not be models adequately. Denitrification is an essential natural nitrogen removal mechanism where $NO3^-$ is converted to gaseous nitrogen by bacteria during anaerobic respiration at the presence of carbon, $NO3^-$ and anoxic condition (Knowles, 1982). Remediation measures, like wetland and detention pond, take advantage of this biogeochemical process in reducing nitrogen pollution. By its nature, denitrification exhibits strong spatial heterogeneity within wetlands and riparian zones where denitrification hot spots are identified (Kaushal & Lewis, 2005; McClain et al., 2003b; McPhillips, Groffman, Goodale, & Walter, 2015; Seitzinger et al., 2006; Shuai, Cardenas, Knappett, Bennett, & Neilson, 2017; Vidon & Hill, 2004). How pollutant and water move along the flow path is crucial to transporting reaction substrate as well as creating suitable soil moisture condition for reactions, while biogeochemical hot spots are the result of the interactions among complementary reactants due to convergence of the flow paths. Without a proper representation of the flow paths and landscape topology, no model can adequately project the hot spots (McClain et al., 2003a). The aforementioned limitations impede efforts for the sound estimation of the level of denitrification as well as its spatial distribution by the currently widely used environmental models.

In recent years, improvements have been made on SWAT for better nitrate-related process simulation. For instance, Hoang et al. (2017) built the model SWAT_LS to enable interactions between upland and riparian zones, and reported enhanced model performance in nitrate simulation. Sun et al. (2017) represented floodplains with a special type of sub-basin and adopted a catena method in SWAT to better represent the role of riverbank buffer strips and wetlands. These models were able to improve nitrate export estimates at the watershed outlets, obtain better overall denitrification results and the characterization of riparian zones as denitrification hotspots at a larger scale. But these improvements are made by tweaks such as including a pre-defined riparian zone or a lowland saturated zone to compensate for the unsatisfactory representation of the surface runoff process and its interactions with the denitrification process. Such tweaks offer limited insights into the mechanism of denitrification and its spatial variations because it is the movement of nitrate meeting organic reducing substrate that creates denitrification hot spots, and not riparian zone itself. Furthermore, within a riparian zone the actual hot spots may occupy only a relatively small area which could even be as small as a few meters wide at the upland margin along flow path (McClain et al., 2003a); (Groffman, Gold, & Simmons, 1992). Ability to pinpoint hot spots in fine scales is important for better management practices. But due to limitations in spatial resolution and model structure, many existing models simply fall short. Thus, attempts to use such models for guiding management plan at a field scale should proceed with caution and proper evaluation before adoption (Wellen et al., 2015).

As a management strategy, it has been proposed to increase nitrogen retention in a watershed by strengthening connection between nitrogen sources and sinks (like wetlands and retention ponds) (Kaushal et al., 2008). In practice, however, it is more cost-effective to focus on critical areas like the riparian zone for their locations and hydrologic connectivity (McClain et al., 2003a), or the areas within the riparian zone where nitrogen, carbon and water co-exist (Clément, Pinay, & Marmonier, 2002). This would require an environmental model that is capable of capturing the mechanism behind the denitrification process and denitrification hotspots at a fine scale. It is needed to further our understanding of the denitrification process and its spatial variation and to provide a sound foundation in improving best management practices. In the meantime, with models like SWAT being widely used, it inevitably brings up the following questions: What kind of uncertainty would such models introduce to the simulated denitrification results by using the oversimplified transport process that has no landscape unit connectivity? What kind of details can such models capture, and what do they miss out? How reliably can we depend on such models to guide management plans like a wetland or retention pond placement? Comparing to SWAT, RHESSys (Regional Hydro-Ecological Simulation System) is a more process-based model which is designed to account for the heterogeneous nature of denitrification and has been also widely used for denitrification modeling (Lin, Webster, Hwang, & Band, 2015; Tague, 2009). But due to lack of studies comparing these different models with well-designed contrast experiments to isolate factors affecting different results, answers to these questions remain elusive. Addressing these important questions is one key impetus of the present study and that requires building appropriate tools.

Objectives of this study are to develop a physically based hydro-environmental model with proper hydrological processes and pollutant transport process for studying NPS nitrogen pollution that not only answers the question of how much nitrate pollutant is generated or removed within a target region, but also provides deeper insights into the complex yet critical denitrification process that affects a watershed's nitrogen cycle dynamics. The hydro-environmental model developed in this study incorporates the biogeochemical processes that are well accepted and made popular by SWAT into relevant hydrological processes. High fidelity representation of landscape is used which is important for capturing the denitrification process that is highly heterogeneous in space and dynamic in time (Osaka et al., 2010; Speiran, 2010). The new model, called DHSVM-N, is built with the Distributed Hydrology Soil and Vegetation Model, DHSVM (Wigmosta, Vail, & Lettenmaier, 1994), which is commonly used for watershed scale hydrology study. In the following, pertinent aspects of DHSVM and SWAT models are further described. How the relevant biogeochemical processes from SWAT are built into DHSVM in this study is detailed next. To explore how the physically based hydrological model affects the environmental modeling outcome, a comparison study using both DHSVM-N and SWAT are employed in studying nitrate export and denitrification over a target watershed. Results are analyzed with focus on patterns of nitrate related processes especially the denitrification process. We further take advantage of the new model, DHSVM-N, and its variant

DHSVM-N_alt to explore uncertainties related to how different representations of the flow path and watershed landscape unit connectivity associated with the transport process would affect the modeling of denitrification process and watershed nitrate export.

2 Methodology

Our hypothesis is that hydrological processes related to soil moisture and runoff play a critical role in affecting nitrate transport and denitrification within a watershed and sufficient rigor in representing these hydrological processes is essential. To test this hypothesis and improve the current state of modeling, we develop a new model that is endowed with adequate functionalities by combining the strengths of DHSVM and SAWT.

2.1 DHSVM and SWAT models in a nutshell

The fundamental differences of these two model structures related to the transport processes are illustrated in Figure 1 (a) and (c). The way water and pollutant travels within a watershed in each model is marked by arrows. Representations of main hydrological processes that are important to soil moisture and flow transport for DHSVM and SWAT are briefly summarized in Table 1. DHSVM is a fully distributed physically based hydrological model which incorporates comprehensive hydrological processes such as evapotranspiration, snow, runoff and streamflow modeling, but it does not include processes related to environmental components such as those related to NSP pollutant transport. SWAT, on the other hand, is a semi-distributed hydro-environmental model with a focus on evaluating impacts of agricultural activities on stream water quality.

In DHSVM, the study domain is divided into grid cells (also called spatial units), each of which is regular shaped and hydrologically connected to its adjacent neighbor cells based on topography, and as a result it can model how water travels among connected cells giving the flow paths which are dictated by topography built from the digital elevation model (DEM) data. DHSVM provides a dynamic representation of the spatial distribution of evapotranspiration, soil moisture, snow cover, and runoff continuously within a study period at the spatial resolution of a given DEM data. Its important features include: 1) both energy and water balance equations are solved simultaneously at each time step for every modeling grid cell in the watershed; 2) evapotranspiration is represented using a two-layer canopy model; 3) both infiltration excess runoff and saturation excess runoff processes are modeled, and the generated overland flow can also be re-infiltrated into other modeling grids along its downslope overland flow path following the topographic landscape; 4) the surface runoff and subsurface runoff are routed separately by the routing processes following the flow path determined by the topography; and 5) runoff from each individual modeling cell is hydrologically linked through both surface and subsurface flow routing algorithms. DHSVM has been widely used for diverse studies at the watershed scale under rain, snow and mixed climatic regimes (Beckers, Smerdon, & Wilson, 2009). For example, Whitaker et al. (2003) evaluated DHSVM's performance on modeling hydrology of a forested watershed using water table depth as an indicator to investigate the model's ability to produce saturation overland flow and reported an overall satisfactory performance. Cuo et al. (2006) reported well modeled root zone soil moisture result at four measurement sites in an experimental watershed in Thailand. Cuartas et al. (2012) applied DHSVM to a lowland tropical rainforest environment and obtained reasonable performance on predicting soil moisture and discharge. Du et al. (2014) reported overall reasonable soil water content modeling results at the surface soil layer (top 60 cm) for a range of canopy conditions in a forest watershed. Ma et al. (2020) reported good spatial-temporal distribution of soil moisture simulation results for determination of agricultural early warning indexes. Yearsley et al. modifies DHSVM with a stream temperature model included to study impact of hydrology and land use on water temperature (Yearsley, Sun, Baptiste, & Nijssen, 2019). Zhang et al. uses DHSVM for soil moisture modeling to monitor impact of waterlogging for crops (Zhang, Yuan, Liu, Gao, & Wang, 2022).

In contrast, the hydrological processes involved in SWAT are much simplified: SWAT divides a watershed into independent and spatially disconnected hydrological response units (HRUs) based on land cover, soil type and slope. There is no substance exchange among the disjointed HRUs. The hydrological and nutrient processes are calculated for each HRU and the resulting flow (both water and nutrients) is routed directly into stream channels skipping the overland flow routing process (i.e., there is no flow travels over the land surface) as depicted in Figure 1(c). Such a representation is inadequate as it cannot account for interactions between the HRUs. In addition, SWAT adopts the empirical curve number (CN) method for runoff generation. The empirical CN method does not properly consider the mechanics of either saturation excess or infiltration excess runoff generation process, further making it inept to depict runoff-prone area while surface runoff is the main flow process and path to transport pollutant to streams (Wellen et al., 2015).

While good match of SWAT's simulated discharge time series at the catchment outlet can be achieved via adjusting each HUR's contributions without including the proper runoff generation mechanisms and surface runoff routing process, the lack of connectivity and interactions between the watershed spatial components (HRUs) limits SWAT's ability to rationally simulate the transport process overland which has long been identified as a crucial weakness of SWAT (Arnold et al., 2010; Bosch et al., 2010; Gassman et al., 2007; Hoang, van Griensven, et al., 2017; Wellen et al., 2015). Furthermore, potential equifinality, i.e., similar results may arise as a consequence of combinations of different processes and parameters (Beven, 2006)) due to overparameterization, could introduce large amounts of uncertainties (Jones et al., 2019). This could be especially the case when the watershed's internal processes are the focus of the study, while the model is only calibrated at the watershed outlet.

2.2 Spatial pattern of soil moisture with DHSVM

Studies have illustrated the capability of DHSVM in adequately simulating soil moisture time series at discrete locations (Cuo et al., 2006; Du et al., 2014), but investigation of its capability in modeling spatial soil moisture patterns has been significantly limited [Slater et al., 2017; Mar et al., 2020]. This represents an important gap. Because the soil moisture pattern plays a pivotal role in NPS pollutant transport, the credence of DHSVM in this respect is assessed first herein before further model development.

This assessment is conducted by making use of the data collected by our group from a dense multi-hop wireless sensor network (WSN) testbed located at the Audubon Society of Western Pennsylvania (ASWP) Beechwood Farms Nature Reserve. The ASWP testbed is about 20 km northeast of the University of Pittsburgh campus, in Southwestern Pennsylvania. The testbed is within the watershed of East Little Pine Creek (ELPC) which has a drainage area of about 15.8 km^2. At this ASWP testbed, hydrological data (i.e., soil moisture, soil water potential, soil temperature and sap flow) are collected. This testbed, which covers an approximate area of 3000 m^2, includes over 240 sensors that are connected to more than 100 heterogeneous motes [Villalba et al., 2017; Zhong et al., 2018]. These sensors include the soil moisture of EC-5, soil temperature and soil water potential of MPS-1 and MPS-2, and sap flow sensors [Davis et al., 2012a; 2012b; 2012c]. The motes are comprised of MICAz, IRIS and TelosB [Davis et al., 2012c; Navarro et al., 2014]. In addition, several data loggers have been installed along the site to provide a comparative reference to the WSN measurements for the purpose of checking the WSN data quality [Villalba et al., 2017]. Figure 2(a) shows an overview of the WSN testbed and locations of some of its sensors over a hillslope area. DHSVM was setup at a 1-m spatial resolution to simulate the water and energy budgets over a small area where good quality data were collected. The forcing data for DHSVM were retrieved from the Weather underground station BigOak - KPAPITTS399, which is located close to the WSN testbed. Soil samples were taken from the site and the soil porosity was then measured at our laboratory. The soil layer depths of DHSVM were set at 0.05, 0.10, 0.30, 0.50, and 1 m, respectively, based on the preliminary onsite information. Other information about the soil and vegetation used in DHSVM was based on the work of Hernandez (Hernández, 2019). To have an objective assessment, no model parameters of DHSVM were calibrated using the testbed sensor data.

Figure 2(b) shows the spatial patterns of soil moisture at 30 cm depth on August 11th, 2016 between the DHSVM model simulations (left) and the data collected from the WSN testbed (right). It can be seen that the spatial pattern from DHSVM is wetter at the foot of the hillslope, but overall, it compares quite well to that from the observations. Figure 2(c) – (e) shows the time series comparisons on soil moisture between DHSVM results and the observed data at three sensor nodes at 10 cm (node 2133) and at 30 cm depth (nodes 2084 and node 2015). In addition, evapotranspiration is also compared between DHSVM results and those calculated based on the sap flow measurements at node 2084 as shown in Figure 2(f). The DHSVM modeled soil moistures, in terms of its magnitude range and trends, agree with the sensor measurements from the WSN testbed albeit some existing gaps and outliers (mainly due to battery power shortage) in the sensor data. Finally, sap flow data collected from node 2084 was converted to plant transpiration and compared to the DHSVM modeled evapotranspiration at the node location (see Figure 2(f)). It is observed that the modeled evapotranspiration is higher than the observed transpiration, but the temporal behavior over the diurnal cycles between the two agrees with each other quite well. The mismatch in magnitudes observed could be due to factors related to the deficiency of DHSVM and the uncertainties involved in the WSN sap flow data collections and the converting factors related to tree properties from sap flow to transpiration. But these results taken as a whole provide credence for DHSVM for capturing the spatial pattern of soil moisture.

2.3 Integration of biogeochemical processes with hydrological processes

DHSVM-N, extends the functionalities of DHSVM to: (1) enable the dynamic plant growth based on temperature, water and nutrient availability to capture the interaction between plant and nutrient type pollutants; (2) enable modeling of nitrogen-related biogeochemical processes in the soil profile; and (3) enable nitrate transport to be integrated with DHSVM's surface/subsurface runoff routing processes.

The original DHSVM uses simple functions to relate the LAI aspect of plant growth and the monthly albedo variation based on a predefined database for each plant type as its biological process representation. We replace them with the method used in SWAT featuring a more dynamic plant growth that accounts for factors like temperature, water and nutrient availability. The biogeochemical and nitrogen-related processes of DHSVM-N are adapted from SWAT as well. That is, the biogeochemical processes of SWAT (e.g., nitrogen-related processes) are integrated with the hydrological processes of DHSVM to form DHSVM-N. The structure of the new DHSVM-N is illustrated in Figure 3. The integration of SWAT's biological and biogeochemical processes into DHSVM involves extensive and substantial changes to the original DHSVM model which include model inputs, structure of impacted process functions, and model outputs. One important motivation of developing this new model, DHSVM-N, based on SWAT's relevant functions, instead of using other existing models, e.g., RHESSys, is that the DHSVM-N model so developed allows us to isolate processes and identify factors regarding what could be the sources of potential different outcomes between DHSVM-N and SWAT.

As shown in Figure 3, the biological and biogeochemical functions introduced to the DHSVM model consist of three main components: plant growth, nitrate transport, and soil biogeochemical processes. In the computational sequence, the runoff and soil moisture are first calculated at an hourly time step based on the original DHSVM hydrological processes and their relevant functions. They are then used as inputs to functions that calculate plant growth and nitrogen-related processes at a daily time step as these processes have slower dynamic responses than those related to water and energy fluxes involved in the original DHSVM model. These plant growth and nitrogen-related processes include decomposition/mineralization of organic nitrogen, plant uptake of nitrate, denitrification, and nitrate transport.

For the dissolved nitrogen (i.e., nitrate in this study) transport with runoff, DHSVM-N assumes a simple complete mixing condition within each time step and the computed nitrate is moved to the connected downstream neighboring grids based on local dissolved nitrate concentration and the amount of runoff outflow. The nitrogen process in streams is simplified by assuming that all nitrate entering stream channels exits the watershed within a short period of time, and that it undergoes no further biogeochemical reactions. These assumptions are based on the fact that a small watershed generally has a short residence time (e.g., within one day) of the stream water in its channel network and that DHSVM-N is typically applied to small scale watershed study. Such assumptions can, however, easily be relaxed if desired or when the DHSVM-N model is applied to a large watershed.

3 Study site and calibration

3.1 Study site and data

The Cane Creek watershed is chosen as a study site for this work because of its rich available data. Its drainage area is 19.58 km^2 located in Orange County, North Carolina. Its primary landcover types are forest (70%) and grasslands (15%). Mean annual temperature is about 14℃ and mean annual precipitation is about 1,170 mm. Figure 4(a) and (b) shows the spatial distributions of its land covers and slopes. This small watershed features a shallow permeable soil layer over a restricting layer and the average soil depth is about 1 m ~ 3 m. Variable source area (VSA) can be used to characterize its surface runoff behavior caused by saturation excess runoff mechanism which accounts for a small portion of the watershed, but its size can be expanded or contracted depending on climate and other hydrological conditions.

DHSVM-N works at a fine resolution of 28 m for each modeling grid cell to capture details in variation in topography, land cover and soils property. To minimize differences that may be caused by spatial resolution between DHSVM-N and SWAT, the HRU delineation of SWAT is selected accordingly which results in a total of 604 HRUs for the study as shown in Figure 4(c) as further increasing in the number of HRUs shows no gain in model performance.

Four years of meteorological data collected by Ameriflux and NOAA from 2007 to 2010 are used as forcing data for both models. The first year is used to calibrate the hydrological model parameters, and the following three years are used for hydrological model validation. The validation uses stream discharge and water quality data collected by USGS.

3.2 Hydrological model calibration

Hydrologically related parameters could not be shared between these two models because of the vast differences in the way each model simulates evapotranspiration, runoff, soil moisture, and overland flow and its flow routing process. These parameters are calibrated separately for the two models based on the same observations from the USGS gauge. The empirical approach in runoff generation and routing of the SWAT model gives it an edge over DHSVM-N in better matching flow discharge observations at the catchment outlet: SWAT tunes the flow discharge contributions from each HRU, and parameters like curve numbers can be easily adjusted to directly affect the total runoff generated. DHSVM, on the other hand, is physically-based and its calibration is carried out by tuning parameters related to soil properties that affect hydrological processes—the room for adjustment is narrow as soil properties have physical bounds. While it is effective to tune SWAT's parameters to match the streamflow observations at the catchment outlet, DHSVM-N, on the other hand, is capable of providing spatial information of the model simulated quantities, such as state variables (e.g., soil moisture), overland flow fluxes, and evapotranspiration, over the entire watershed. Thus, DHSVM-N has an advantage over SWAT when the focus of the study also includes the quantities occurring at inner locations within the watershed.

Figure 4(f) shows stream discharge results from DHSVM-N and SWAT. The Nash–Sutcliffe Efficiency (NSE) is used to compare daily simulated discharge with measurements. NSE is defined as,

$$NSE = 1 - \frac{\sum_t \left(Q_m^t - Q_0^t\right)^2}{\sum_t \left(Q_0^t - \bar{Q}_0\right)^2} \quad (1)$$

Q_m^t: modeled discharge at time t,

Q_0^t: observed discharge at time t,

$\bar{Q}_0$: average observed discharge over s study period.

NSE for DHSVM-N and SWAT during the calibration period (2007) is 0.54 (DHSVM-N) and 0.56 (SWAT), respectively, and during the validation period (2008-2010) is 0.56 (DHSVM-N) and 0.65 (SWAT), respectively. The goodness-of-fit over the calibration period is about the same for DHSVM-N and SWAT, with SWAT fairs better during the validation period which can be attributed to the fact that NSE is more dominated by the peak discharge fit which SAWT does better where the simplification in SWAT has less impact on the peak discharge simulations in this sample. DHSVM-N, however, yields better results during the low flow period over the validation period. We deem current stream discharge results are good enough for carrying out nitrogen process simulations and that setting up comparisons between nitrogen modeling results of the two models would not introduce significant biases nor would they alter the insights from the comparison studies.

3.3 Nitrate loading and initial condition setting

To investigate impacts of the hydrological processes on the spatial distribution of denitrification and the nitrate transport process due to the nature of NPS pollution, a high and a low loading scenario are considered for both models. For the low loading scenario, 1.5 ppm nitrate (equivalent to 14.5 kg N/ha/yr on average for 2007 – 2010) is evenly added to the watershed via precipitation. For a high loading scenario, an extra 82.3 kg N/ha/yr nitrate is evenly divided and added to the watershed surface at the start of each month from February to July. Quantities of all nitrogen species are initiated at the start of the first year (2007) so that the two models start with the same amount of total nitrogen in the soil layer. Additionally, organic carbon is assumed to be uniformly distributed in space across the study watershed for both SWAT and DHSVM-N.

4 Construct of DHSVM-N_Alt

When nitrogen enters the watershed as a NPS pollutant via precipitation or fertilization, the dissolvable nitrate follows a transport process associated with the movement of water. This process is complicated. On one hand, the physical-chemical process such as sorption of dissolved pollutant to soil particles can affect the pollutant's mobility, transport velocity and retention in the watershed (Brusseau, 1994; Cvetkovic & Dagan, 1994; Hrachowitz et al., 2016);

on the other, the chemical, biological (i.e., degradation) and bio-physical processes (i.e., uptake by plant/microbes) can simultaneously affect the fate of the pollutant by altering its form or taking it out of its flow medium (Fatichi, Pappas, & Ivanov, 2016; Galloway et al., 2003; Wexler, Goodale, McGuire, Bailey, & Groffman, 2014). This is why a good environmental model in the present context should combine both to capture the nature of the transport process in a meaningful way (Rinaldo et al., 2015).

After entering a watershed, nitrate keeps interacting with its ambient environment along its pathways, they may be reduced owing to consumption by plant uptake and denitrification, or increased due to decomposition/mineralization. It is, therefore, incorrect to assume mass conservation for nitrate within a watershed. How and to what extent that nitrate interacts with the environment depend on the local environmental conditions, including factors such as soil moisture, reactant availability, plant types, residence time of water, and their spatial heterogeneity.

Most environmental models, as exemplified by SWAT, focus on how fast nitrate travels across the landscape in the watershed to streams and neglect the pathways along which nitrate travels to the streams. By routing nitrate directly to stream channels from individual spatial units, nitrate transport component of such models is revised in an empirical manner: Traveling velocity or retention time of nitrate during the transport process is estimated based on the flux of water. This is quite unsatisfactory and especially problematic as the heterogeneous nature of denitrification processes can in no way be so accounted.

These two different ways of modeling nitrate transport by DHSVM-N and SWAT are further illustrated in Figures 1 (b) and 1 (c). DHSVM-N follows what happens along the flow pathways dictated by topography and considers interactions between nitrate and its environment along its pathways. Spatial variations of the environmental conditions including varying temperature, soil moisture and availability of complementary reaction substrates are considered in DHSVM-N, leading to a better representation of various heterogeneous and dynamic biogeochemical processes.

The substantial differences in the model constructs of DHSVM-N and SWAT make it infeasible to isolate the sole impacts of transport methods used between them. It is under this context that a variant of DHSVM-N, called DHSVM-N_alt, is introduced so that meaningful comparison experiments can be performed to highlight the role of the transport process on denitrification modeling results. DHSVM-N_alt is basically constructed the same way as DHSVM-N except that its nitrate transport model is replaced by that resembles the method used in SWAT as shown in Figure 1 (d). That is, in DHSVM-N_alt nitrate is discharged directly to stream channels from each spatial unit using an empirical nitrate transport equation listed below as Eq. (2), which is applied both to the over land surface nitrate that moves with the surface runoff and to the nitrate in the soils that moves with the subsurface flow in the saturated zone. This equation is modified from SWAT (Neitsch, Arnold, Kiniry, & Williams, 2011) in which the amount of nitrate exported to stream channel from a given grid over time is obtained as follows,

$$NO3_{surf} = NO3'_{surf} \times \frac{Q_{out}}{Q_{total}} \times C_1 + NO3'_{surf-1} \times C_2 \tag{2}$$

$NO3_{surf}$: amount of nitrate discharged to stream channel on a given day [kg N/ha]

$NO3'_{surf}$: amount of nitrate in runoff of a given grid [kg N/ha]

$NO3'_{surf-1}$: amount of nitrate lagged from previous day [kg N/ha]

Q_{out}: amount of runoff flows out of a given grid [mm H_2O]

Q_{total} : amount of total runoff generated at a given grid [mm H_2O]

C_1: calibration parameter controlling amount of $NO3'_{surf}$ discharged directly to stream

C_2: calibration parameter controlling amount of $NO3'_{surf-1}$ discharged directly to stream

The surface and subsurface nitrate transport processes have different C_1 and C_2 coefficients.

Through calibration, DHSVM-N_alt is made to yield similar overall nitrate retention time and nitrate export capacity as does by DHSVM-N. Both models use the same set of parameters except that DHSVM-N_alt has introduced Eq (2) additionally. The calibration procedure is carried out as follows: 1) nitrogen-related transformative biogeochemical processes are turned off for both models; 2) DHSVM-N is run first and gives nitrate export time series at the watershed outlet; 3) DHSVM-N_alt is calibrated by tuning C_1 and C_2 until it gives compatible nitrate export time series. After the calibration, the nitrogen-related transformative biogeochemical processes are turned back on for both models for analysis to start.

DHSVM-N_alt and DHSVM-N only differ in that DHSVM-N_alt has nitrate continuously removed from each spatial unit for the amount that flow directly into stream channels based on Eq. (2) during a run. There are no differences in runoff, soil moisture and stream discharge results. Whatever differences in the results between these two models can be attributed to the part due to nitrate transport directly to streams as taken by SWAT.

Calibration of DHSVM-N_alt's transport equation is carried out assuming 10.0 ppm nitrate in rainfall as the sole nitrate source for the time period 2007 – 2010. This gives C_1=0.38 and C_2=0.4 for the surface nitrate transport; and C_1=0.005 and C_2=0.7 for the subsurface nitrate transport. The calibration is deemed satisfactory as the results from DHSVM-N_alt compare well with those from DHSVM-N as depicted in Figure 4 (d) with $R^2 = 0.91$.

After calibration, DHSVM-N_alt is run under the same conditions and setup as laid out in Section 3.

5 Results and discussion

Results from DHSVM-N, SWAT and DHSVM-N_alt are compared here in terms of total nitrate export, soil moisture distribution, decomposition and mineralization of organic nitrogen, and denitrification.

5.1 Total nitrate export

For the nitrogen model simulations, DHSVM-N and SWAT are given the same set of parameters that control nitrogen-plant-soil cycle. Figure 4(e) shows modeled nitrate stream export results on days USGS monitoring data are available, assuming the measurements were collected under a condition similar to our low nitrate loading scenario. In general, the two models perform similarly on those days. However, most USGS observations are collected during normal or low flow period, and there is lack of observations during peak discharge period -- which is the nitrate export hot moment, as shown in a recent study by Lu et. al (2020) that heavy storm events can attribute to as high as one third of the total nitrate export. Results from these two models differ significantly during the critical peak discharge periods as shown in Figure 4 (g), indicating very different underlying nitrogen dynamics being simulated by the two models. Part of the differences can be attributed to less nitrate plant uptake and less efficient process of denitrification in SWAT (see Table 2), and leading SWAT to have more nitrate export at the watershed outlet.

Table 2 compares nitrate mass balance obtained over the modeling time period from 2008 to 2010. For DHSVM-N, the two major nitrate sources for the low nitrate loading scenarios are nitrate in rainfall and nitrate from decomposition/mineralization of organic nitrogen. For the high loading scenario, denitrification and plant uptake consume up to a total of 112.7 kg N/ha/yr nitrate which far exceeds nitrate via natural rainfall process (15.6 kg N/ha/yr) and decomposition/mineralization process (22.7 kg N/ha/yr), strongly suggesting that the extra nitrate loading acting as main source of nitrate for various processes. Comparing with DHSVM-N, SWAT result shows less decomposition/mineralization and denitrification activities under both nitrate loading scenarios. However, while SWAT generates less nitrate plant uptake (14.5 kg N/ha/yr) under the low loading case, its results under the high loading case (31.7 kg N/ha/yr) exceed that from DHSVM-N (18.2 kg N/ha/yr). Possible explanation is that for DHSVM-N under the high loading case plants compete for a more efficient denitrification process for the nitrate source.

Overall DHSVM-N shows higher nitrate originated from decomposition/mineralization process than SWAT. Nitrogen decomposition/mineralization processes are related to soil moisture, and therefore the differences in the results can be explained by the different soil moisture results from the two models, which are discussed later. DHSVM-N also shows much higher denitrification compared to SWAT (11.3 kg N/ha/yr compared to 1.6 kg N/ha/yr). Both the wetter soil condition as shown in Figure 5 (a) and the advantage of better representing denitrification hot spots by DHSVM-N (see Figure 6 (a) right) contribute to this result. But the role of each individual aspect remains unknown and is a focus of discussion in a later part of this paper. Having a larger source of nitrate from enhanced decomposition/mineralization processes in DHSVM-N also partially contributes to this result. This is especially the case for the low nitrate loading scenario where decomposition/mineralization process is a main nitrate source aside from the nitrate in precipitation (as shown in Table 2). The higher denitrification activity and plant uptake modeled by DHSVM-N explains lower stream nitrate export compared to the SWAT's result.

5.2 Soil moisture distribution

Soil moisture is a key factor in many nitrogen-related processes, and the distinct ways that these two models incorporate the hydrologic processes yield very different soil moisture distributions, which, in turn, affect the outcome of nitrogen-related processes.

The soil moisture threshold for initiating denitrification is set at the field capacity for both SWAT and DHSVM-N. Overall, higher soil moisture content means a higher chance of triggering denitrification process across the watershed. Higher soil moisture also enhances decomposition and mineralization of organic nitrogen to produce more soil nitrate which can be denitrified later. Figure 5(a) shows spatial patterns of relative soil moisture in the root zone (the top 1.2 m of soil in this study) transitioning from a wet period to a relatively dry period for both models. In general, the soil moisture tends to be higher in non-forest area (i.e., grass, shrub, and cropland) for both models due to lower evapotranspiration from these plants. Results from DHSVM-N show an overall higher relative soil moisture transitioning from its areal average of 0.91 to 0.78 compared to that from 0.78 to 0.60 in SWAT. DHSVM-N shows much higher soil moisture in the valleys and lowland areas, where saturation excess runoff often occurs, than that in the other areas of the watershed. Such a spatial distribution of the soil moisture is consistent to the watershed characteristics where soil moisture saturation zones are distributed along valleys and flow pathways dictated by the topography. DHSVM-N also better captures the evolution of saturated zones than SWAT during this transition period with a gradual contraction. In SWAT, its soil moisture distribution is mainly linked to land cover and soil properties and does not capture the spatial distribution/patterns of the saturated areas (see Fig. 5a). By utilizing high resolution DEM, DHSVM-N can model the spatial patterns of denitrification in a more detailed fashion as discuss later.

5.3 Decomposition and mineralization of organic nitrogen

Decomposition/mineralization process breaks fresh residue from plant droppings or complex organic nitrogen into simpler mineral forms. Environmental factors affecting these processes include temperature, availability of organic nitrogen and soil moisture. DHSVM-N generates more nitrate than SWAT from such a decomposition/mineralization process as summarized in Table 2. For the low loading scenario, DHSVM-N generates 100.0% more nitrate than does SWAT while for the high loading scenario, it is only 34% more (Table 2). Spatial patterns of the generated nitrate from the decomposition/mineralization process are shown in Figure 5(b) for the low nitrate loading case. Both models show similar spatial patterns for the hot spots (i.e., locations with high generated nitrate values) but their magnitudes are quite different. These hot spots correspond to the cropland areas which are marked in orange color in the SWAT map and in red color in the DHSVM-N map in Figure 5(b). The spatial patterns and distribution for the forest and grass/shrub areas (i.e., non-hot spots) are also similar between the two models with DHSVM-N produces again higher nitrate numbers. The lower nitrate numbers in SWAT than those in DHSVM-N are mainly caused by the lower soil moisture obtained in SWAT as shown in Figure 5(a), while the similar spatial patterns (see Figure 5(b)) are mainly due to the spatial distributions of the different vegetation types (see Figure 4(a)). In other words, the spatial patterns here are controlled by the vegetation types while the magnitudes are mainly affected by the soil moisture.

5.4 Denitrification

Denitrification, a key natural nitrate removal process, has been found to exhibit large spatial heterogeneity in many studies (Kaushal & Lewis, 2005; McClain et al., 2003b; McPhillips et al., 2015; Seitzinger et al., 2006; Vidon & Hill, 2004). Locations within a watershed that yield unproportionally high level of denitrification activity are often referred to as denitrification “hot spots”. Because of the complex nature of denitrification process, it has been challenging in the past to correctly pinpoint such “hot spots” via modeling. Both SWAT and DHSVM-N are examined for their ability to capture the spatial distribution of denitrification herein. Figure 6 depicts the spatial patterns of total denitrification for the study period in 3D plots with z-axis showing total amount of denitrification over the modeling period. The elevation of the terrain is exaggerated to highlight the terrain.

5.4.1 Denitrification spatial pattern from SWAT

SWAT gives two different denitrification spatial patterns depending on the nitrate loading levels. For the low nitrate loading scenario as shown in Figure 6(a), its denitrification features a clear pattern that is linked mostly to land cover types: the forest area has the least overall denitrification activity compared to non-forested grass land area.

Decomposition/mineralization of organic nitrogen, such as leaf residual, plays a much bigger role in supplying nitrate for denitrification process with 8.6 kg N/ha/yr nitrate produced annually (see Table 2), which accounts for 35.5% of the total available nitrate, compared to that in the high loading case where decomposition/mineralization only explains 14.7% of the total available nitrate. This is further observed by comparing Figure 6(a) and Figure 5(b). They show that denitrification hot spots also happen to be the decomposition/mineralization hot spots, suggesting that the denitrification spatial pattern is strongly linked to the distribution of available nitrate source. These results are consistent with the study by Ferrant et al. (2011) which shows a similar link between the denitrification pattern and land cover with SWAT. Such an outcome is a direct consequence that SWAT associates soil moisture and nitrate availability with land cover type and soil type (David et al., 2009).

For the high nitrate loading scenario as shown in Figure 6(b), denitrification pattern from the SWAT results is no longer tied to land cover, due to the dominant effect of large amount of nitrate loading being spatially homogeneously applied across the watershed. The main source of nitrate for denitrification has shifted to the extra loaded nitrate, which accounts for 82.3 kg N/ha/yr nitrate as potential reactant to the denitrification process. Even though nitrate generated from decomposition/mineralization has increased to 16.9 kg N/ha/yr (see Table 2), this is still too little compared to the amount loaded from the external nitrate source (82.3 kg N/ha/yr). Thus, the spatial variation of the denitrification pattern is completely masked by the large amount of nitrate added through external nitrate loading which has a homogeneous spatial distribution. As a result, denitrification spatial pattern from SWAT is no longer limited by the availability of nitrate source as in the low loading scenario. Since SWAT fails to produce significant spatial heterogeneity in soil moisture distribution (see Figure 5(a)), the overall denitrification spatial pattern becomes much more homogeneous (see Figure 6(b)) compared to the low nitrate loading scenario (Figure 6(a)) where the land cover type causes discernable impact.

In general, such SWAT results run contrary to the denitrification spatial patterns typically observed in the fields which are found highly spatially heterogeneous with “hot spots” existed in areas like wetland, riparian zone or along flow pathways (Kaushal & Lewis, 2005; McClain et al., 2003b; McPhillips et al., 2015; Seitzinger et al., 2006; Shuai et al., 2017; Vidon & Hill, 2004). Failure to reflect what has been observed in the fields calls into question on the use of SWAT in investigating the denitrification process and thereby limits its applicability to make agricultural and environmental management plans when sensitive denitrification hot spots need to be located/identified.

The overall drier soil condition computed by SWAT also means that less overall denitrification is obtained compared to the results from DHSVM-N. Although there is a lack of observations for validation on this front, underestimated soil moisture by SWAT has been reported (Rajib, Golden, Lane, & Wu, 2020). Given that the physically- and hydrologically-based processes involved in a watershed tend to be over-simplified in SWAT and that there are a large number of model parameters which can be adjusted through model calibration, there is a potential for SWAT to obtain the right results using unreasonable parameter combinations due to the fallacy of equifinality (Evenson, Golden, Lane, & D'Amico, 2016; Jones et al., 2019). Thus, study results on denitrification based on SWAT's simulations should be carefully analyzed and use with prudence, especially when not enough observations are available to validate the spatial distribution of its soil moisture.

5.4.2 Denitrification spatial pattern from DHSVM-N

DHSVM-N yields overall higher total denitrification across the study region with 11.3 and 94.5 kg N/ha/yr for both the low and high nitrate loading scenarios, respectively. This can be attributed to its higher soil moisture which facilitates the denitrification process. The elevated soil moisture also enhances organic nitrogen decomposition/mineralization processes which adds additional nitrate supply for denitrification.

The most significant differences between SWAT and DHSVM-N are the denitrification's spatial distribution and patterns for scenarios with both the low and high loadings as shown in Figure 6(a) and 6(b). Under the low nitrate loading case, results from DHSVM-N in Figure 6(a) show a clear pattern of denitrification "hot spots", represented by the red "sticks", which are located either next to the main stream riverbanks, along major flow pathways, or concentrated in the landscape's depressions. Beaujouan et al. (2002) showed similar results using a process-based model called TNT2 to account for spatial interactions. While their study only involved a hypothetical catchment of a rectangular shape and simple assumptions on land cover and soil type to test effects of different topography and landscape scenarios, results of Beaujouan et al. (2002) yielded spatial patterns similar to those from DHSVM-N, indicating denitrification hot spots concentrated around downslope or depression areas are due to topography and spatial interactions. Li et al. (2018) and Zhu et al. [2010] also found that topography accounts for a large part of the denitrification spatial heterogeneity through field observations and measurements. Similar conclusions can further be found in literature(Kaushal & Lewis, 2005; McClain et al., 2003b; McPhillips et al., 2015; Seitzinger et al., 2006; Shuai et al., 2017; Vidon & Hill, 2004). In addition to the spatial patterns impacted and induced by topography, DHSVM-N shows that land cover and plant type also contribute to the spatial heterogeneity of denitrification. Similar to SWAT, non-forest areas in DHSVM-N tend to have relatively higher denitrification activities. In short, for the low nitrate loading case, results from DHSVM-N suggest that there is a strong link between terrain and the spatial pattern of denitrification for hot spots aside from the impact of different land cover type while SWAT does not show such a link.

For the high nitrate loading scenario as shown in Figure 6(b), the external nitrate loading which is homogeneously distributed in space also plays a dominant role in supplying nitrate to the denitrification process in DHSVM-N. Similar to SWAT, the high nitrate loading has eliminated most of the heterogeneity introduced by the different types of land cover as those orange patches shown in Figure 6(a) for DHSVM-N disappear in Figure 6(b). However, contrary to SWAT, one can clearly see that much higher level of denitrification activities still takes place along the flow pathways and in the riparian zones, as shown by the red “sticks” (i.e., hot spots) in Figure 6(b), which are similar to those shown in the low loading scenario. A further investigation of the sources for the difference between SWAT and DHSVM-N is provided by DHSVM-N_alt which is presented in later discussion. Another noticeable difference between SWAT and DHSVM-N, as shown in Table 2, is that SWAT obtains much higher nitrate absorbed by plant (31.7 kg N/ha/yr) under the high loading scenario compared to DHSVM-N (18.2 kg N/ha/yr). This difference is attributed to the fact that DHSVM-N obtains much higher denitrification (94.5 kg N/ha/yr as opposed to 31.2 kg N/ha/yr in SWAT) and therefore there is less nitrate available for the plant to absorb.

In summary, for both the low and high loadings, locations of the denitrification “hot spots” manifested by DHSVM-N are closely linked to the flow pathways related to hillslopes and to the riparian zones along the main channels, all of which are determined by the topography. Such a result is consistent with the findings from field measurements by Zhu et al. (2010) and the study by Shabaga and Hill (2010) who had also identified that the denitrification hotspots were located along flow pathways. To better illustrate the role of topography in the nitrate’s overland flow transport, we also have placed nitrate sources at different locations and study where the transport process would lead them. Such results are illustrated in Figure 7. Nitrate originated from different sources as observed clearly follows the landscape terrain to reach the stream channels as indicated by the green paths. These different flow paths which are naturally associated with different characteristics, such as length, slope, soil wetness, surface permeability, and plant species and robustness of microbe activity, together not only affect the movement of nitrate but also decide the biogeochemical process that nitrate is involved in. By considering detailed information of such transport flow paths interactions between the transport and biogeochemical reactions the denitrification processes can then be dynamically and realistically represented. Therefore, topography, which determines the flow pathways, plays a crucial role in how nitrate spreads out over land and takes part in its various reactions before reaching the stream channels. But a question remains: would the denitrification be simulated differently if such a flow path is not incorporated into the nitrate transport method? This is addressed next.

5.5 Impacts of landscape spatial connectivity on nitrate transport

Table 3 summarizes the similarities and differences in the model construct among DHSVM-N, DHSVM-N_alt and SWAT. One can expect that DHSVM-N_alt to produce similar results as those from DHSVM-N on spatial distributions and magnitudes of the soil moisture, surface runoff and other fluxes. Differences in the transport methods between these two models (see Table 3) are the main source that will lead to the differences in results between these two models. As shown in Table 2, between DHSVM-N and DHSVM-N_alt, their major differences are in the nitrate removal by denitrification and the nitrate stream export. For example, the DHSVM-N and DHSVM-N_alt give, respectively, 7.6 kg N/ha/yr (51.9% less than SWAT) and 12.6 kg N/ha/yr (20.2% less than SWAT) stream nitrate export from 2008 to 2010 for the high loading case; and 2.0 kg N/ha/yr (20.0% less than SWAT) and 2.6 kg N/ha/yr (4.0% more than SWAT) stream nitrate export, respectively, for the low loading case. As for denitrification, DHSVM-N and DHSVM-N_alt report 11.3 kg N/ha/yr and 10.9 kg N/ha/yr, respectively, in the low loading scenario, and 94.5 kg N/ha/yr and 89.4 kg N/ha/yr, respectively, in the high loading scenario. Although the differences in total amount of the denitrification are small between the two models, i.e., 11.3 kg/ha/yr (DHSVM-N) vs. 10.9 kg/ha/yr (DHSVM-N_alt) for the low loading, and 94.5 kg/ha/yr (DHSVM-N) vs. 89.4 kg/ha/yr (DHSVM-N) for the high loading, it is the spatial distributions of denitrification, as shown in Figure 6, that is where the differences really lie.

More specifically, under the low nitrate loading scenario, the land cover type affects denitrification pattern with the non-forest type generally gives higher denitrification (Fig. 6a). Although DHSVM-N and DHSVM-N_alt show similar denitrification spot distribution for most parts of the watershed as well as similar total denitrification amount due to their similarity in the hydrological processes (see Table 3), but at locations with high denitrification they are dramatically different. In that, DHSVM-N clearly demonstrating hot spots (defined as locations with denitrification greater than 24.0 kg N/ha/yr) locate along the flow pathways and around the riparian zones, while DHSVM-N_alt showing no hot spots at all just like SWAT (Fig. 6a). With this comparison between DHSVM-N and DHSVM-N_alt, we are able to show that the routing approach used in SWAT and other environmental models could miss "hot spot" in their application. This clearly illustrates the profound importance of the role the nitrate routing methods play.

In addition to the identification of denitrification hot spots, the influence of other locations with high denitrification capacity is also investigated Table 4 summarized the significance of such impact with DHSVM-N model. Furthermore, the modeling grids whose denitrification amount is greater than the highest top 1.0% based on the denitrification data histogram are computed. For the low loading case, this relatively high denitrification area amounts to 1.0% of the watershed area and contributes to 3.7% of the total quantity of denitrification. However, if the denitrification capabilities by these grids are not identified or ignored or not adequately modeled, they can potentially lead to as much as 20.0% increase in the stream nitrate export if all such unconsumed nitrate enters the stream channels for the low nitrate loading case. These same grids, on the other hand, would only cause as little as 0.8% and 3.8% stream nitrate export increase in SWAT and DHSVM-N_alt, respectively, as indicated in Table 4, portraying a potentially significantly biased and mis-leading picture on the stream nitrate export.

For the high loading case, the excessive external source of nitrate applied homogeneously to the watershed "masks" or overrides the impact of the land cover types on the denitrification's spatial patterns, and thus results in an overall more homogeneous spatial pattern of denitrification as shown in Fig 6. Still, only DHSVM-N can identify denitrification hot spots (defined as locations with denitrification greater than 200.0 kg N/ha/yr) along the flow pathways and around the riparian zone while both SWAT and DHSVM-N_alt cannot (Figure 6). In addition, a failure in simulating these hot spots and other relatively high denitrification locations, which together comprise the top 1.0% highest denitrification areas identified in DHSVM-N, would potentially cause as much as 38.2% of increase in the stream nitrate export if all such unconsumed nitrate entered the stream channels as in a worst-case scenario, despite that these locations together only account for 3.1% of the total denitrification amount. For SWAT and DHSVM-N_alt, the amount of denitrification from these same locations would account for 1.4% and 0.7%, respectively, of their total denitrification amount which would only lead to a minor increase in the stream nitrate export of just 2.5% for SWAT and 4.8% for DHSVM-N_alt as shown in Table 4. From both Figure 6 and Table 4, we can see that impacts of these high-denitrification-capacity locations in the high nitrate loading case are similar to those for the low loading case. The reason that DHSVM-N is capable of simulating these denitrification locations and also the hot spots in both loading scenarios while DNSVM-N_alt and SWAT cannot is that DHSVM-N's transport model is fundamentally different from DHSVM-N_alt and SWAT while the latter two share the same transport method. In other words, the construct of DHSVM-N_alt demonstrates what the critical factor or the essential cause is in determining a model's capability of simulating the hot spots. Analysis here demonstrates that significantly different conclusions, which would lead to different best management plan and strategy, could be drawn from different models depending on which transport approach (i.e., the routing method) these models use, and therefore, decision makers should be careful with the tools they use when making their management planning.

It is also worth pointing out that DHSVM-N and DHSVM-N_alt yield very similar total denitrification results in both low and high loading scenarios, and both are drastically different from the SWAT's result. Considering annual nitrate flux where the sources of nitrate include rainfall, external nitrate (e.g., fertilizer) and decomposition/mineralization while the nitrate sinks include plant uptake, stream export and denitrification, for SWAT, there are 5.6 kg N/ha/yr (15.6 + 8.6 - 14.5 - 1.6 - 2.5 = 5.6) and 36.1 kg N/ha/yr (15.6 + 82.3 + 16.9 - 31.7 – 31.2 -15.8 = 36.1) annual nitrate accumulation within the system for low and high loading scenarios, respectively; for DHSVM-N_alt, the annual nitrate accumulation value is only 0.8 kg N/ha/yr (15.6 + 17.0 - 18.3 – 10.9 – 2.6 = 0.8) and 0.4 kg N/ha/yr (15.6 + 82.3 + 22.6 – 18.1 – 89.4 – 12.6 = 0.4) for low and high loading scenarios, respectively. The high amount of unconsumed nitrate in SWAT suggests that the denitrification process in SWAT is unlikely limited by nitrate availability.

Given that the soil carbon distributions are the same and that the two models transport the nitrate in a similar way (i.e., directly to the outlet from its modeling unit), it clearly implies that the enhanced denitrification in DHSVM-N_alt compared to SWAT is due to its very different hydrology consideration that gives much wetter soil moisture. This stresses the importance of the impact of hydrological processes on affecting the denitrification simulation process. For identification of the spatial patterns of denitrification or pinpointing down sensitive denitrification hot spots and not just the stream water quality, a realistic nitrate transport method like the one adopted by DHSVM-N is necessary since the lateral flow of nitrate plays a more predominant role. Many widely used environmental models with over-simplified model structures would be thus inadequate because they are not designed to accommodate hot spots computation which is a key to a watershed management at the field scale (Wellen et al., 2015). Even if one is able to obtain high quality soil moisture observation data (typically not available at present) and incorporate them into the model's calibration process to improve the soil moisture simulation of SWAT, the over-simplified transport process of SWAT would still significantly mis-represent the important denitrification hot spots which would introduce sufficient errors to affect the management decision making process. This is an aspect that is commonly overlooked in the decision-making process, but its importance is well showcased in our study here.

Furthermore, for optimizing efficiency of a treatment facility, it is crucial that a model capable of accounting for impacts of the hydrological flow pathways on biogeochemical processes is employed so that locations where pollutant from a large contributing area converges as the result of the transport process can be identified and selected as potentially good ones for building a treatment facility. This may only be achieved via models like DHSVM-N that link pollution source and sink with a more realistic transport method (i.e., routing method) which is capable of representing the landscape topology and connectivity. Investigation results on this issue will be reported at its due course in the near future.

6 Conclusions

To demonstrate and address the inadequacy of the current hydro-environmental models such as the widely adopted SWAT in studying NPS nitrate transport and denitrification problems, a new model, DHSVM-N, is developed in this study. Among the most critical drawbacks of SWAT is the omission of landscape connectivity, namely, surface runoff generated from one area does not go through its downslope neighboring land, but rather directly goes to the streams. Secondly, adequate representations of important hydrological processes, such as surface runoff generation, re-infiltration process, and evapotranspiration, are necessary to obtain adequate soil moisture and its spatial distribution as soil moisture plays an important role in the biogeochemical processes such as decomposition and mineralization, plant uptake, and denitrification. DHSVM-N is developed by fuse the best features of SWAT with those of a fully distributed physically based hydrological model, DHSVM, together with improvement on the nitrate transport related processes.

From the comparison studies carried out, results from the new model, DHSVM-N, show that it is pivotal to have a physically based hydrological model that is properly connected to a high-resolution landscape-based routing model to adequately represent the relevant hydrological processes and transport (i.e., routing) process as they significantly affect the denitrification process and the nitrate transport. The new model is demonstrated being capable of giving watershed denitrification spatial pattern and denitrification “hot spots” in fine detail that better match findings in the literature and observations made in the field. This suggests a great potential of this new model in pinpointing down sensitive areas involved in environmental issues, advising people in agricultural management practices, and prioritizing environmental conservation plans. On the other hand, although SWAT has been a powerful and popular environmental modeling tool on larger scale studies and will continue to be widely used, its over-simplified hydrological processes and lack of landscape connectivity representation limit its use beyond stream water quality in certain scenarios. This is particularly so because unless flow pathways and biochemical processes along the flow paths are adequately incorporated, hydro-environmental models such as SWAT are ill-equipped to provide reasonable estimate to processes like denitrification which is associated with great spatial heterogeneity. Environmental studies where hydrological processes play crucial roles would be prudent to examine the adequacy of the hydrological processes represented in their models and the types of problems the models are capable of addressing. We show here where the SWAT model comes up short and why our new model, DHSVM-N, needs to be developed.

We have also constructed a variant version of DHSVM-N called DHSVM-N_alt for the purpose of investigating how the factors such as nitrate transport modeling, representation of landscape connectivity, flow paths and hydrology modeling may impact the denitrification study outcomes. Comparison study using this alternate shows without ambiguity that hydrology modeling is critical in obtaining the overall denitrification pattern (except for hot spots) across a watershed. Their impacts are manifested through the levels of soil moisture within a watershed which is central in various biogeochemical processes and the amount of surface runoff generated which determines the mobility and pathways of nitrate. Landscape topology and connectivity involved in the transport modeling part determines how nitrate is redistributed over land. While it does not impact the overall picture of the nitrogen process modeled as shown by DHSVM-N_alt (see Figure 6), the landscape topology and its associated connectivity play a crucial role in modeling the hot spots of the denitrification process, and therefore can be crucial for management practices. In short, nitrate does not jump from a location of the landscape directly into streams, and thus it should not be so modeled especially when specific management practice at a field scale is to be designed with the model simulation results. Depending on the goals of a study, models incapable of incorporating this detail in its transport method may yield unrealistic results for denitrification, and thus have severe limitations on their usefulness in real world applications. The hydro-environmental model developed in this study demonstrates how such shortcomings of existing models may introduce uncertainties to results as well as how they can be circumvented and amended. Results of this study provide model users insights to help them select the right tools based on the models' strengths and limitations given the tasks at hand.

Acknowledgments:

This work was partially supported by the U.S. National Science Foundation under CBET-1236403 and CNS-1319331 to the University of Pittsburgh, and by the William Kepler

Whiteford Professorship to Xu Liang from the University of Pittsburgh. We also thank the Center for Research Computing and the Swanson School of Engineering of the University of Pittsburgh for providing the computational resources.

Author contributions:

For this work, Y. Wen implemented the research ideas, developed DHSVM-N and DHSVM-N_alt models, performed model simulation experiments, conducted analysis, prepared most of the figures, and co-wrote the manuscript. J-S Lin analyzed and synthesized the results, and co-wrote the manuscript. F. Plaza prepared Figure 2 and contributed to the writing of Section 2.2. X. Liang conceived the research ideas, supervised the investigation, analyzed and synthesized the results, and co-wrote and finalized the manuscript. Wen, Lin, and Liang contributed to the design of the model simulation experiments. All contributed to the discussions of the work.

Data access:

Data used in this study is from NOAA (https://www.noaa.gov/), Ameriflux (https://ameriflux.lbl.gov/) and USDA Web Soil Survey (https://websoilsurvey.sc.egov.usda.gov/). DHSVM model (https://dhsvm.pnnl.gov/) is open-source.

Open Research:

No.

References

Arnold, J., Allen, P., Volk, M., Williams, J., & Bosch, D. (2010). Assessment of different representations of spatial variability on SWAT model performance. *Transactions of the ASABE, 53*(5), 1433-1443.

Beaujouan, V., Durand, P., Ruiz, L., Aurousseau, P., & Cotteret, G. (2002). A hydrological model dedicated to topography-based simulation of nitrogen transfer and transformation: rationale and application to the geomorphology– denitrification relationship. *Hydrological Processes, 16*(2), 493-507. doi:https://doi.org/10.1002/hyp.327

Beckers, J., Smerdon, B., & Wilson, M. (2009). Review of hydrologic models for forest management and climate change applications in British Columbia and Alberta. forrex Forum for Research and Extension in Natural Resources, Kamloops, BC forrex Series 25. *British Columbia, Canada*, 29-38.

Beven, K. (2006). A manifesto for the equifinality thesis. *Journal of hydrology, 320*(1-2), 18-36.

Bosch, D., Arnold, J., Volk, M., & Allen, P. (2010). Simulation of a low-gradient coastal plain watershed using the SWAT landscape model. *Transactions of the ASABE, 53*(5), 1445-1456.

Brusseau, M. L. (1994). Transport of reactive contaminants in heterogeneous porous media. *Reviews of Geophysics, 32*(3), 285-313.

Clément, J. C., Pinay, G., & Marmonier, P. (2002). Seasonal dynamics of denitrification along topohydrosequences in three different riparian wetlands. *Journal of Environmental Quality, 31*(3), 1025-1037.

Cuartas, L. A., Tomasella, J., Nobre, A. D., Nobre, C. A., Hodnett, M. G., Waterloo, M. J., . . . Ferreira, M. (2012). Distributed hydrological modeling of a micro-scale rainforest watershed in Amazonia: Model evaluation and advances in calibration using the new HAND terrain model. *Journal of hydrology, 462-463*, 15-27. doi:https://doi.org/10.1016/j.jhydrol.2011.12.047

Cuo, L., Giambelluca, T. W., Ziegler, A. D., & Nullet, M. A. (2006). Use of the distributed hydrology soil vegetation model to study road effects on hydrological processes in Pang Khum Experimental Watershed, northern Thailand. *Forest Ecology and Management, 224*(1-2), 81-94.

Cvetkovic, V., & Dagan, G. (1994). Transport of kinetically sorbing solute by steady random velocity in heterogeneous porous formations. *Journal of Fluid Mechanics, 265*, 189-215.

David, M. B., Del Grosso, S. J., Hu, X., Marshall, E. P., McIsaac, G. F., Parton, W. J., . . . Youssef, M. A. (2009). Modeling denitrification in a tile-drained, corn and soybean agroecosystem of Illinois, USA. *Biogeochemistry, 93*(1-2), 7-30.

Du, E., Link, T. E., Gravelle, J. A., & Hubbart, J. A. (2014). Validation and sensitivity test of the distributed hydrology soil-vegetation model (DHSVM) in a forested mountain watershed. *Hydrological Processes, 28*(26), 6196-6210.

Easton, Z. M., Fuka, D. R., Walter, M. T., Cowan, D. M., Schneiderman, E. M., & Steenhuis, T. S. (2008). Re-conceptualizing the soil and water assessment tool (SWAT) model to predict runoff from variable source areas. *Journal of hydrology, 348*(3-4), 279-291.

EEA. (2007). *Europe's environment: the fourth assessment*: Office for Official Publ. of the European Communities.

EPA, U. (2002). The National Water Quality Inventory: Report to Congress for the 2002 Reporting Cycle–A Profile. *Washington, DC.: United States Environmental Protection Agency (EPA)*.

Evenson, G. R., Golden, H. E., Lane, C. R., & D'Amico, E. (2016). An improved representation of geographically isolated wetlands in a watershed-scale hydrologic model. *Hydrological Processes, 30*(22), 4168-4184.

Fatichi, S., Pappas, C., & Ivanov, V. Y. (2016). Modeling plant–water interactions: an ecohydrological overview from the cell to the global scale. *Wiley Interdisciplinary Reviews: Water, 3*(3), 327-368.

Ferrant, S., Oehler, F., Durand, P., Ruiz, L., Salmon-Monviola, J., Justes, E., . . . Sanchez-Perez, J.-M. (2011). Understanding nitrogen transfer dynamics in a small agricultural catchment: Comparison of a distributed (TNT2) and a semi distributed (SWAT) modeling approaches. *Journal of hydrology, 406*(1-2), 1-15.

Galloway, J. N., Aber, J. D., Erisman, J. W., Seitzinger, S. P., Howarth, R. W., Cowling, E. B., & Cosby, B. J. (2003). The nitrogen cascade. *Bioscience, 53*(4), 341-356.

Gassman, P. W., Reyes, M. R., Green, C. H., & Arnold, J. G. (2007). The soil and water assessment tool: historical development, applications, and future research directions. *Transactions of the ASABE, 50*(4), 1211-1250.

Groffman, P. M., Gold, A. J., & Simmons, R. C. (1992). *Nitrate dynamics in riparian forests: microbial studies* (0047-2425). Retrieved from

Hernández, F. (2019). *Integrated High-Resolution Modeling for Operational Hydrologic Forecasting*. University of Pittsburgh.

Hoang, L., Schneiderman, E. M., Moore, K. E., Mukundan, R., Owens, E. M., & Steenhuis, T. S. (2017). Predicting saturation-excess runoff distribution with a lumped hillslope model: SWAT-HS. *Hydrological Processes, 31*(12), 2226-2243.

Hoang, L., van Griensven, A., & Mynett, A. (2017). Enhancing the SWAT model for simulating denitrification in riparian zones at the river basin scale. *Environmental Modelling & Software, 93*, 163-179.

Hrachowitz, M., Benettin, P., Van Breukelen, B. M., Fovet, O., Howden, N. J., Ruiz, L., . . . Wade, A. J. (2016). Transit times—the link between hydrology and water quality at the catchment scale. *Wiley Interdisciplinary Reviews: Water, 3*(5), 629-657.

Jones, C. N., Ameli, A., Neff, B. P., Evenson, G. R., McLaughlin, D. L., Golden, H. E., & Lane, C. R. (2019). Modeling connectivity of non-floodplain wetlands: Insights, approaches, and recommendations. *JAWRA Journal of the American Water Resources Association, 55*(3), 559-577.

Kaushal, S. S., Groffman, P. M., Band, L. E., Shields, C. A., Morgan, R. P., Palmer, M. A., . . . Fisher, G. T. (2008). Interaction between urbanization and climate variability amplifies watershed nitrate export in Maryland. *Environmental science & technology, 42*(16), 5872-5878.

Kaushal, S. S., & Lewis, W. M. (2005). Fate and transport of organic nitrogen in minimally disturbed montane streams of Colorado, USA. *Biogeochemistry, 74*(3), 303-321.

Knowles, R. (1982). Denitrification. *Microbiological reviews, 46*(1), 43-70.

Li, X., McCarty, G. W., Lang, M., Ducey, T., Hunt, P., & Miller, J. (2018). Topographic and physicochemical controls on soil denitrification in prior converted croplands located on the Delmarva Peninsula, USA. *Geoderma, 309*, 41-49. doi:https://doi.org/10.1016/j.geoderma.2017.09.003

Lin, L., Webster, J. R., Hwang, T., & Band, L. E. (2015). Effects of lateral nitrate flux and instream processes on dissolved inorganic nitrogen export in a forested catchment: A model sensitivity analysis. *Water resources research, 51*(4), 2680-2695.

Lu, C., Zhang, J., Tian, H., Crumpton, W. G., Helmers, M. J., Cai, W.-J., . . . Lohrenz, S. E. (2020). Increased extreme precipitation challenges nitrogen load management to the Gulf of Mexico. *Communications Earth & Environment, 1*(1), 1-10.

Ma, Y., Xiong, Q., Zhu, J., & Jiang, S. (2020). Early warning indexes determination of the crop injuries caused by waterlogging based on DHSVM model. *The Journal of Supercomputing, 76*(4), 2435-2448.

McClain, M. E., Boyer, E. W., Dent, C. L., Gergel, S. E., Grimm, N. B., Groffman, P. M., . . . Mayorga, E. (2003a). Biogeochemical hot spots and hot moments at the interface of terrestrial and aquatic ecosystems. *Ecosystems*, 301-312.

McClain, M. E., Boyer, E. W., Dent, C. L., Gergel, S. E., Grimm, N. B., Groffman, P. M., . . . Mayorga, E. (2003b). Biogeochemical hot spots and hot moments at the interface of terrestrial and aquatic ecosystems. *Ecosystems, 6*(4), 301-312.

McPhillips, L. E., Groffman, P. M., Goodale, C. L., & Walter, M. T. (2015). Hydrologic and biogeochemical drivers of riparian denitrification in an agricultural watershed. *Water, Air, & Soil Pollution, 226*(6), 169.

Mitchell, M. J. (2001). Linkages of nitrate losses in watersheds to hydrological processes. *Hydrological Processes, 15*(17), 3305-3307.

Neitsch, S. L., Arnold, J. G., Kiniry, J. R., & Williams, J. R. (2011). *Soil and water assessment tool theoretical documentation version 2009*. Retrieved from

Ongley, E. D., Xiaolan, Z., & Tao, Y. (2010). Current status of agricultural and rural non-point source pollution assessment in China. *Environmental Pollution, 158*(5), 1159-1168.

Osaka, K. i., Ohte, N., Koba, K., Yoshimizu, C., Katsuyama, M., Tani, M., . . . Nagata, T. (2010). Hydrological influences on spatiotemporal variations of δ15N and δ18O of nitrate in a forested headwater catchment in central Japan: Denitrification plays a critical role in groundwater. *Journal of Geophysical Research: Biogeosciences, 115*(G2).

Rajib, A., Golden, H. E., Lane, C. R., & Wu, Q. (2020). Surface depression and wetland water storage improves major river basin hydrologic predictions. *Water resources research, 56*(7), e2019WR026561.

Rinaldo, A., Benettin, P., Harman, C. J., Hrachowitz, M., McGuire, K. J., Van Der Velde, Y., . . . Botter, G. (2015). Storage selection functions: A coherent framework for quantifying how catchments store and release water and solutes. *Water resources research, 51*(6), 4840-4847.

Seitzinger, S., Harrison, J. A., Böhlke, J., Bouwman, A., Lowrance, R., Peterson, B., . . . Drecht, G. V. (2006). Denitrification across landscapes and waterscapes: a synthesis. *Ecological Applications, 16*(6), 2064-2090.

Shabaga, J. A., & Hill, A. R. (2010). Groundwater-fed surface flow path hydrodynamics and nitrate removal in three riparian zones in southern Ontario, Canada. *Journal of hydrology, 388*(1-2), 52-64.

Shen, Z., Liao, Q., Hong, Q., & Gong, Y. (2012). An overview of research on agricultural non-point source pollution modelling in China. *Separation and Purification Technology, 84*, 104-111.

Shuai, P., Cardenas, M. B., Knappett, P. S., Bennett, P. C., & Neilson, B. T. (2017). Denitrification in the banks of fluctuating rivers: The effects of river stage amplitude, sediment hydraulic conductivity and dispersivity, and ambient groundwater flow. *Water resources research, 53*(9), 7951-7967.

Sinha, E., Michalak, A., & Balaji, V. (2017). Eutrophication will increase during the 21st century as a result of precipitation changes. *Science, 357*(6349), 405-408.

Speiran, G. K. (2010). Effects of Groundwater-Flow Paths On Nitrate Concentrations Across Two Riparian Forest Corridors 1. *JAWRA Journal of the American Water Resources Association, 46*(2), 246-260.

Sun, X., Bernard-Jannin, L., Sauvage, S., Garneau, C., Arnold, J., Srinivasan, R., & Sánchez-Pérez, J. (2017). Assessment of the denitrification process in alluvial wetlands at floodplain scale using the SWAT model. *Ecological Engineering, 103*, 344-358.

Tague, C. (2009). Modeling hydrologic controls on denitrification: sensitivity to parameter uncertainty and landscape representation. *Biogeochemistry, 93*(1), 79-90.

Torres-Martínez, J. A., Mora, A., Mahlknecht, J., Daesslé, L. W., Cervantes-Avilés, P. A., & Ledesma-Ruiz, R. (2021). Estimation of nitrate pollution sources and transformations in groundwater of an intensive livestock-agricultural area (Comarca Lagunera), combining major ions, stable isotopes and MixSIAR model. *Environmental Pollution, 269*, 115445.

Vidon, P., & Hill, A. R. (2004). Denitrification and patterns of electron donors and acceptors in eight riparian zones with contrasting hydrogeology. *Biogeochemistry, 71*(2), 259-283.

Wellen, C., Kamran-Disfani, A.-R., & Arhonditsis, G. B. (2015). Evaluation of the current state of distributed watershed nutrient water quality modeling. *Environmental science & technology, 49*(6), 3278-3290.

Wexler, S. K., Goodale, C. L., McGuire, K. J., Bailey, S. W., & Groffman, P. M. (2014). Isotopic signals of summer denitrification in a northern hardwood forested catchment. *Proceedings of the National Academy of Sciences, 111*(46), 16413-16418.

Whitaker, A., Alila, Y., Beckers, J., & Toews, D. (2003). Application of the distributed hydrology soil vegetation model to Redfish Creek, British Columbia: model evaluation using internal catchment data. *Hydrological Processes, 17*(2), 199-224.

White, E. D., Easton, Z. M., Fuka, D. R., Collick, A. S., Adgo, E., McCartney, M., . . . Steenhuis, T. S. (2011). Development and application of a physically based landscape water balance in the SWAT model. *Hydrological Processes*, *25*(6), 915-925.

Wigmosta, M. S., Vail, L. W., & Lettenmaier, D. P. (1994). A distributed hydrology-vegetation model for complex terrain. *Water resources research*, *30*(6), 1665-1679.

Woodbury, J. D., Shoemaker, C. A., Easton, Z. M., & Cowan, D. M. (2014). Application of SWAT with and without variable source area hydrology to a large watershed. *JAWRA Journal of the American Water Resources Association*, *50*(1), 42-56.

Yearsley, J. R., Sun, N., Baptiste, M., & Nijssen, B. (2019). Assessing the impacts of hydrologic and land use alterations on water temperature in the Farmington River basin in Connecticut. *Hydrology and Earth System Sciences*, *23*(11), 4491-4508.

Zhang, X., Yuan, X., Liu, H., Gao, H., & Wang, X. (2022). Soil Moisture Estimation for Winter-Wheat Waterlogging Monitoring by Assimilating Remote Sensing Inversion Data into the Distributed Hydrology Soil Vegetation Model. *Remote Sensing, 14*(3), 792.

Zhu, J., Mulder, J., & Dörsch, P. (2010). Denitrification and N2O emission in an N-saturated subtropical forest catchment, southwest China. *EGUGA*, 10185.

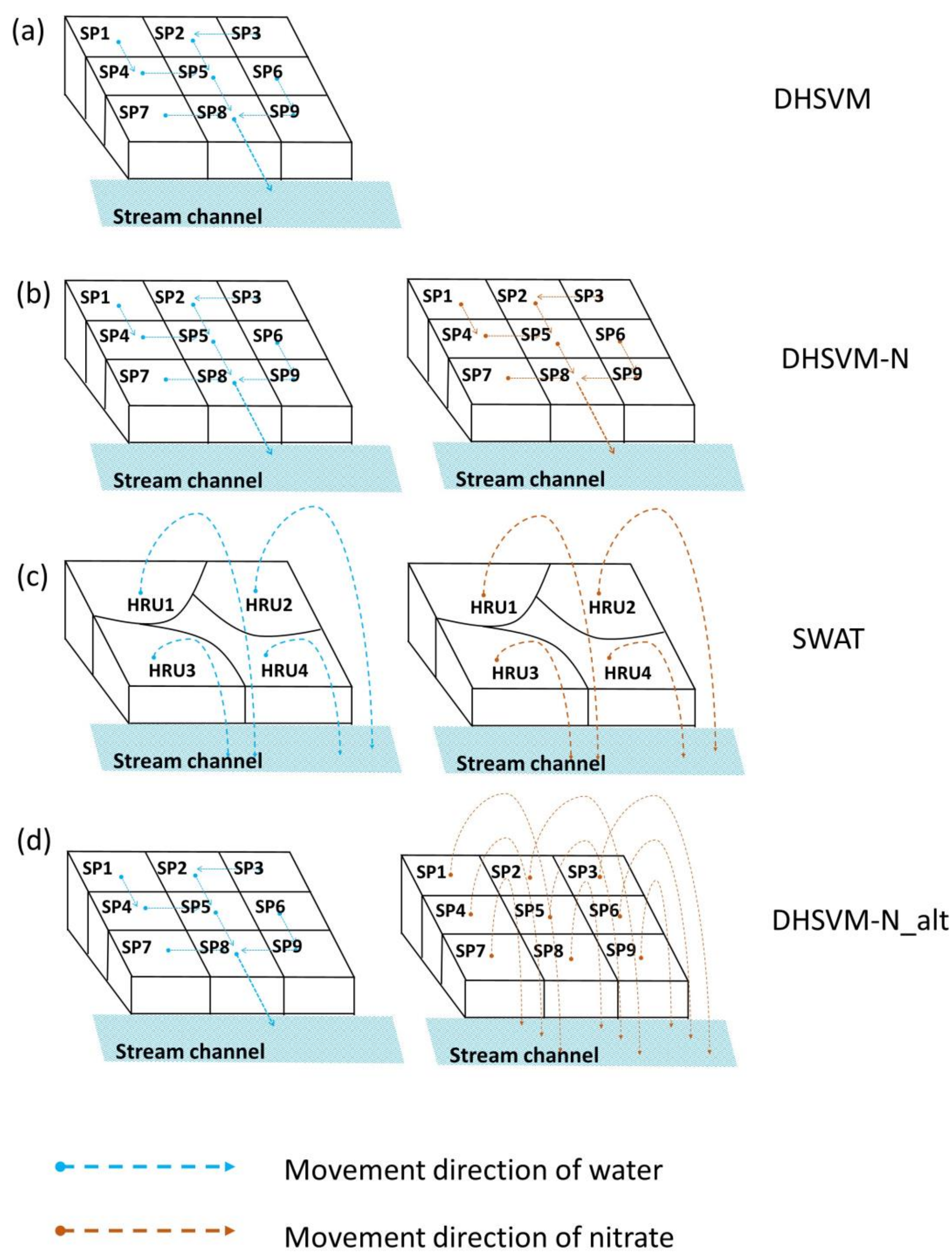
(a)
SP1
SP2
SP3
SP4
SP5
SP6
SP7
SP8
SP9
Stream channel
DHSVM
(b)
DHSVM-N
(c)
HRU1
HRU2
HRU3
HRU4
SWAT
(d)
DHSVM-N_alt
Movement direction of water
Movement direction of nitrate

1086

Figure 1. Spatial unit setup and model structure of (a) DHSVM, (b) DHSVM-N, (c) SWAT, and (d) DHSVM-N_alt. The dashed arrows marked how runoff or nitrate travel to stream channels from each modeling unit. The runoff in both DHSVM and DHSVM-N is routed in the same way to the channel following its flow path, determined by topography, along which the spatial units (i.e., modeling grid cells) can interact with one another through exchange of water, while SWAT has no overland flow routing process involved where the runoff is directly transported to stream. DHSVM-N_alt generates runoff and routes it through the flow network in the same way as it is in DHSVM-N (i.e., left in (d)), but its nitrate transport follows that of SWAT in which the nitrate is directly transported to the stream from each cell. This is achieved by introducing a set of coefficients of C_1 and C_2 (from Eq. 2) to route nitrogen to stream directly with one set for the surface runoff and another set for the subsurface runoff, respectively, to give it a similar travel time and residence time with those from DHSVM-N when nitrogen-related transformative biogeochemical processes are turned off. Note: “SP” here stands for “spatial unit”; HRU is the spatial unit for SWAT.

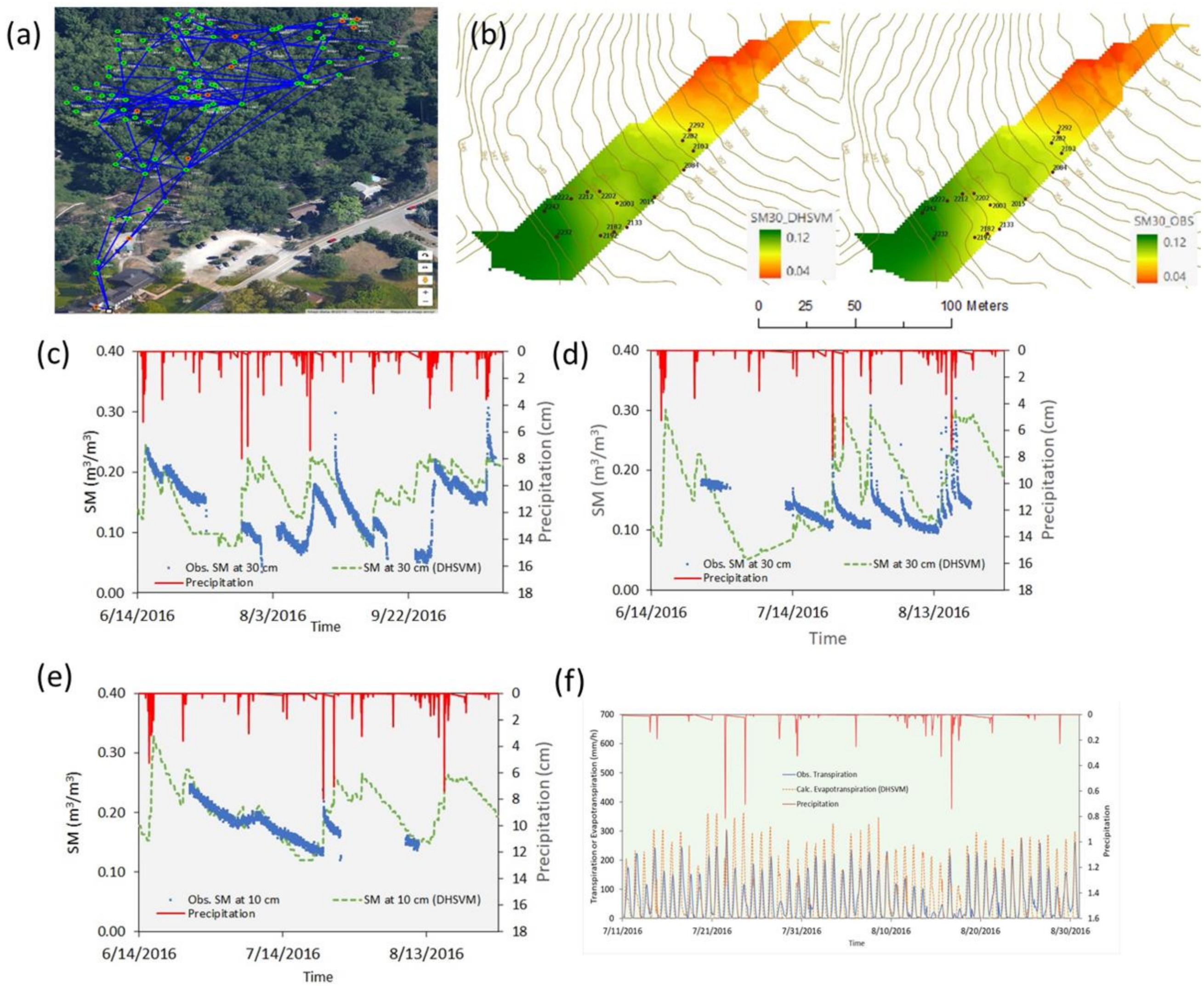

Figure 2. (a) A snapshot of our ASWP WSN testbed (The dots show the locations of the nodes with green or red indicating good or low battery, respectively. The blue lines show the wireless link connectivity between the nodes). (b) Comparison of spatial distribution of daily averaged soil moisture at 30 cm on August 11th, 2016 between DHSVM model simulations (left) and the WSN measurements interpreted using the Kriging method (right). (c) Modeled and observed soil moisture at 30 cm at node 2084 (middle of the hillslope). (d) Modeled and observed soil moisture at 30 cm at node 2015 (between nodes 2084 and 2133). (e) Modeled and observed soil moisture at 10 cm at node 2133 (lower portion of the hillslope). (f) Modeled and observed evapotranspiration at node 2084.

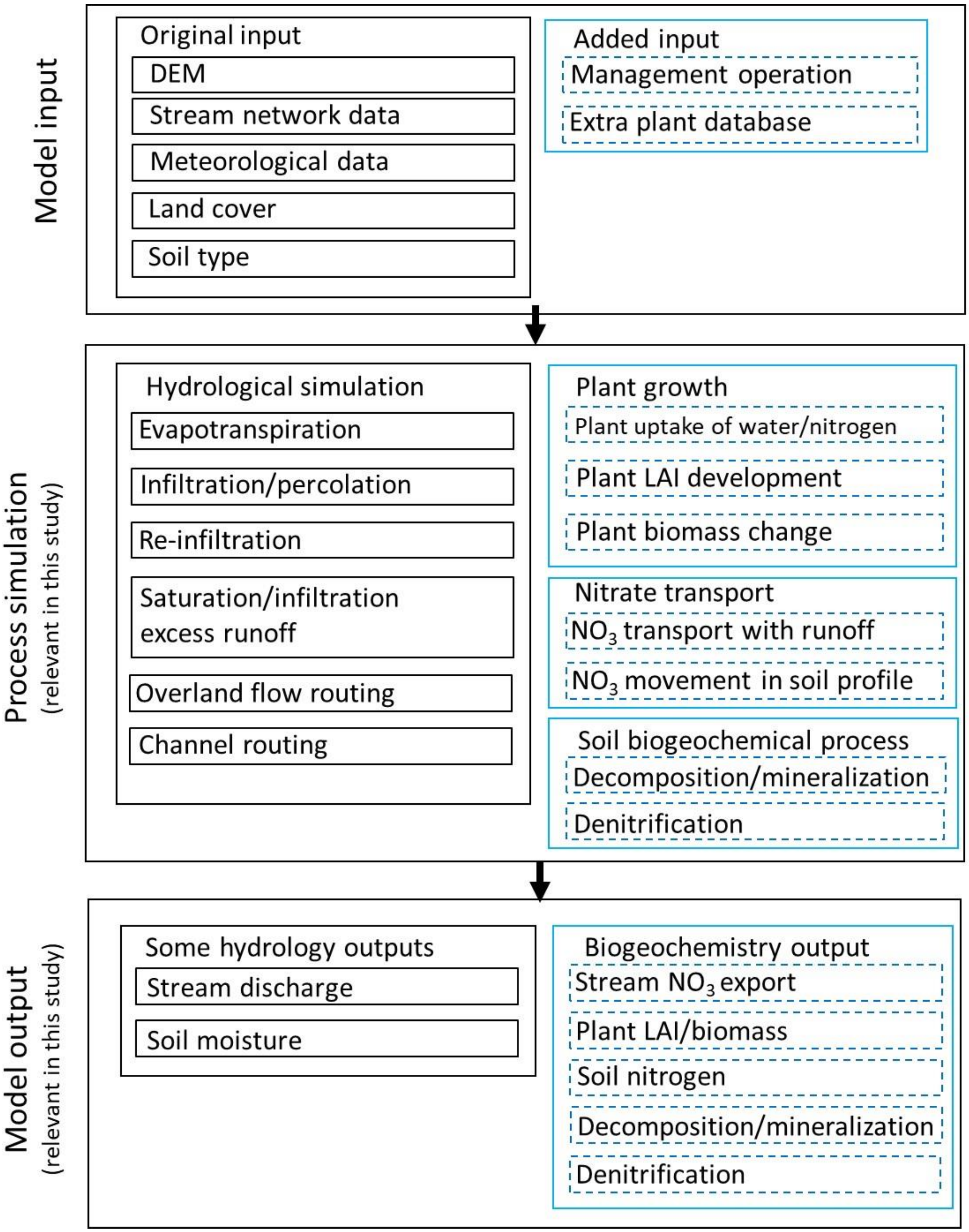

Figure 3. A schematic of DHSVM-N. The parts in blue boxes are functions added to original DHSVM based on methods used in SWAT.

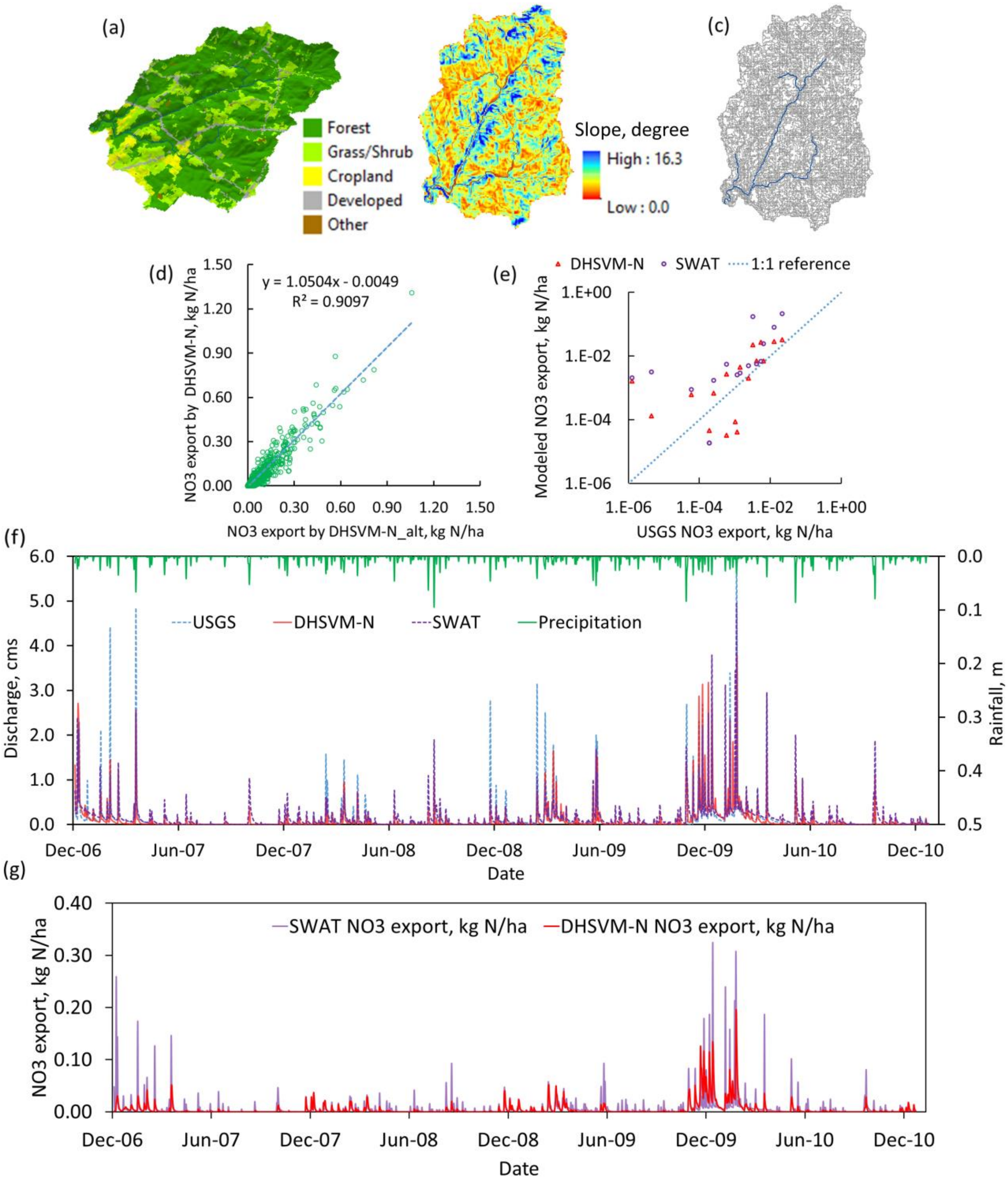

Figure 4. (a) Land cover map for Cane Creek watershed. Most of the watershed is covered by forest (dark green) and the rest is mainly grassland and cropland (light green). (b) Slope map for Cane Creek watershed (unit: degree). The steepest slopes distribute around near main stream channels. (c). Delineated HRU for SWAT model. A total of 604 HRUs are obtained by

overlapping land cover map, soil type map and slope map. Five slope classes are used with emphasis on representing gentle slope area for better denitrification simulation. (d) NO3 export result after calibrating DHSVM-N_alt to match nitrate transport capacity of DHSVM-N without biogeochemical reaction (Result is obtained by assuming 10.0 ppm nitrate in rainfall as the only nitrate source). (e) Watershed nitrate export results from both models plotted against USGS field measurement for the sampling days. (f) Stream discharge modeling results from DHSVM-N and SWAT (plotted against USGS field measurement) using 4 years of daily discharge data. (g) Watershed nitrate export results (plotted against USGS field measurement) for the whole simulation period under natural/low nitrate loading condition (1.5 ppm nitrate in rainfall).

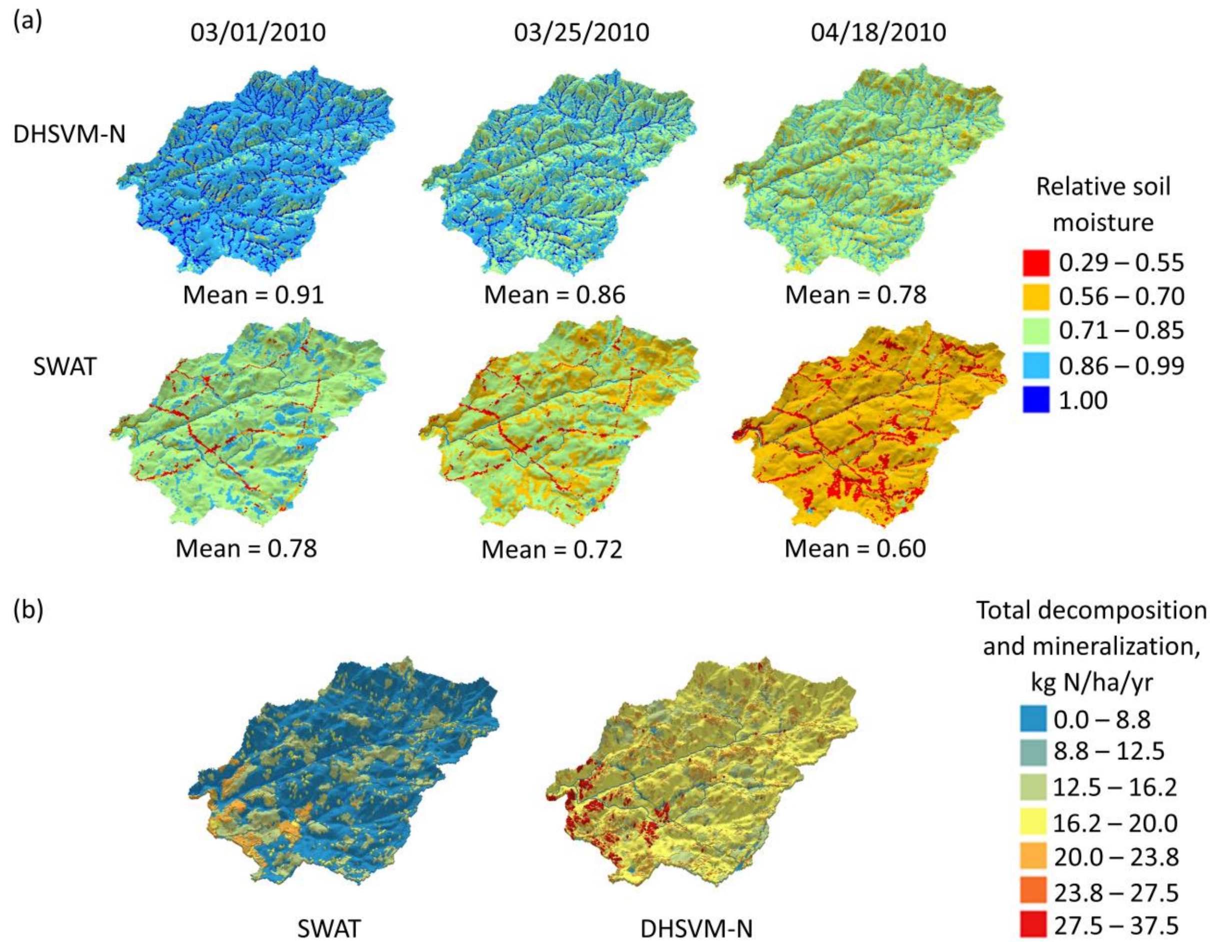

Figure 5. (a) Spatial patterns of relative soil moisture from a wet period transitioning to a drier period based on simulation result from DHSVM-N (upper row) and SWAT (lower row) under natural condition (1.5 ppm nitrate in rainfall). 1.0 indicates soil is at saturation. (b) Spatial patterns of total decomposition and mineralization from SWAT (left) and DHSVM-N (right) under natural condition (1.5 ppm nitrate in rainfall). The elevation is exaggerated to highlight terrain.

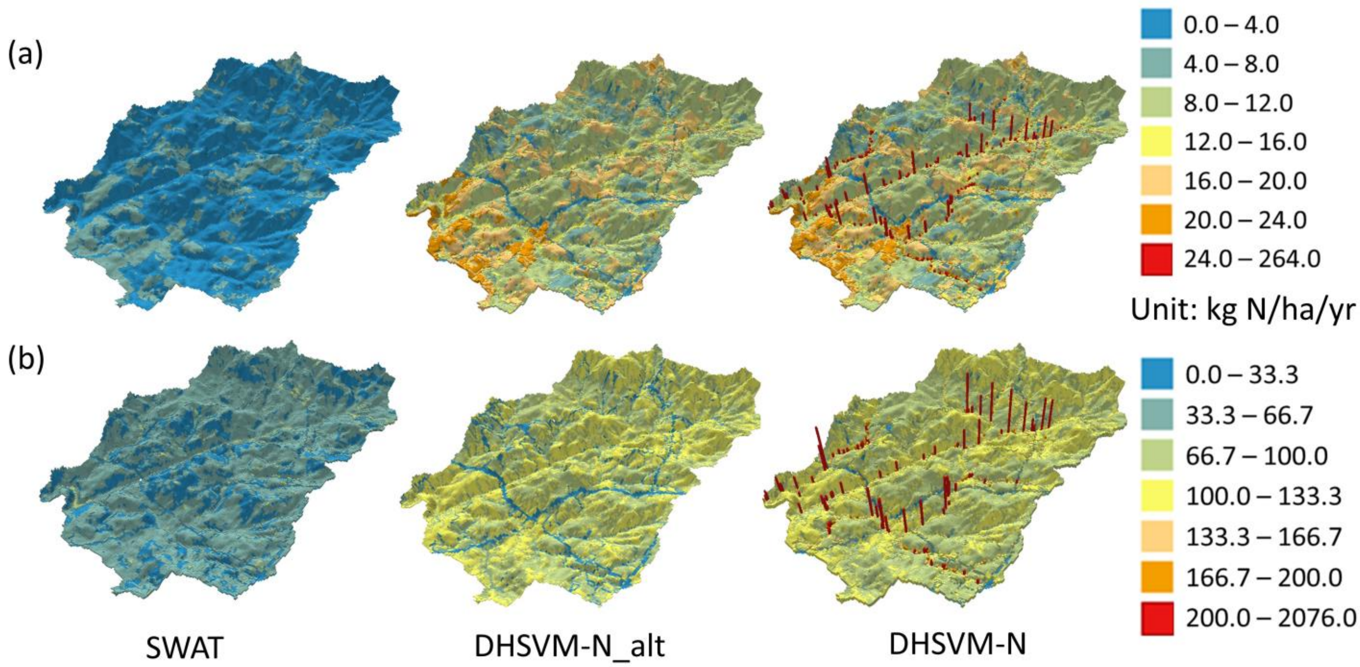

Figure 6. (a) Spatial patterns of total denitrification during the simulation period 2008-2010 based on result from SWAT (left), DHSVM-N_alt (middle) and DHSVM-N (right) for natural nitrate loading condition, i.e., the scenario with 15.6 kg N/ha/yr annual nitrate loading. The z-axis represents absolute value of denitrification. Red "sticks" in the DHSVM-N represent the hot spots since their values are very high as shown by the color scheme. (b) Spatial patterns of total denitrification during the simulation period based on simulation result from SWAT (left), DHSVM-N_alt (middle) and DHSVM-N (right) for high nitrate loading condition, with extra 82.3 kg N/ha/yr annual nitrate loading in addition to 1.5 ppm nitrate in rainfall. The z-axis denotes absolute value of denitrification. Note: terrain is exaggerated to emphasize locations of valley.

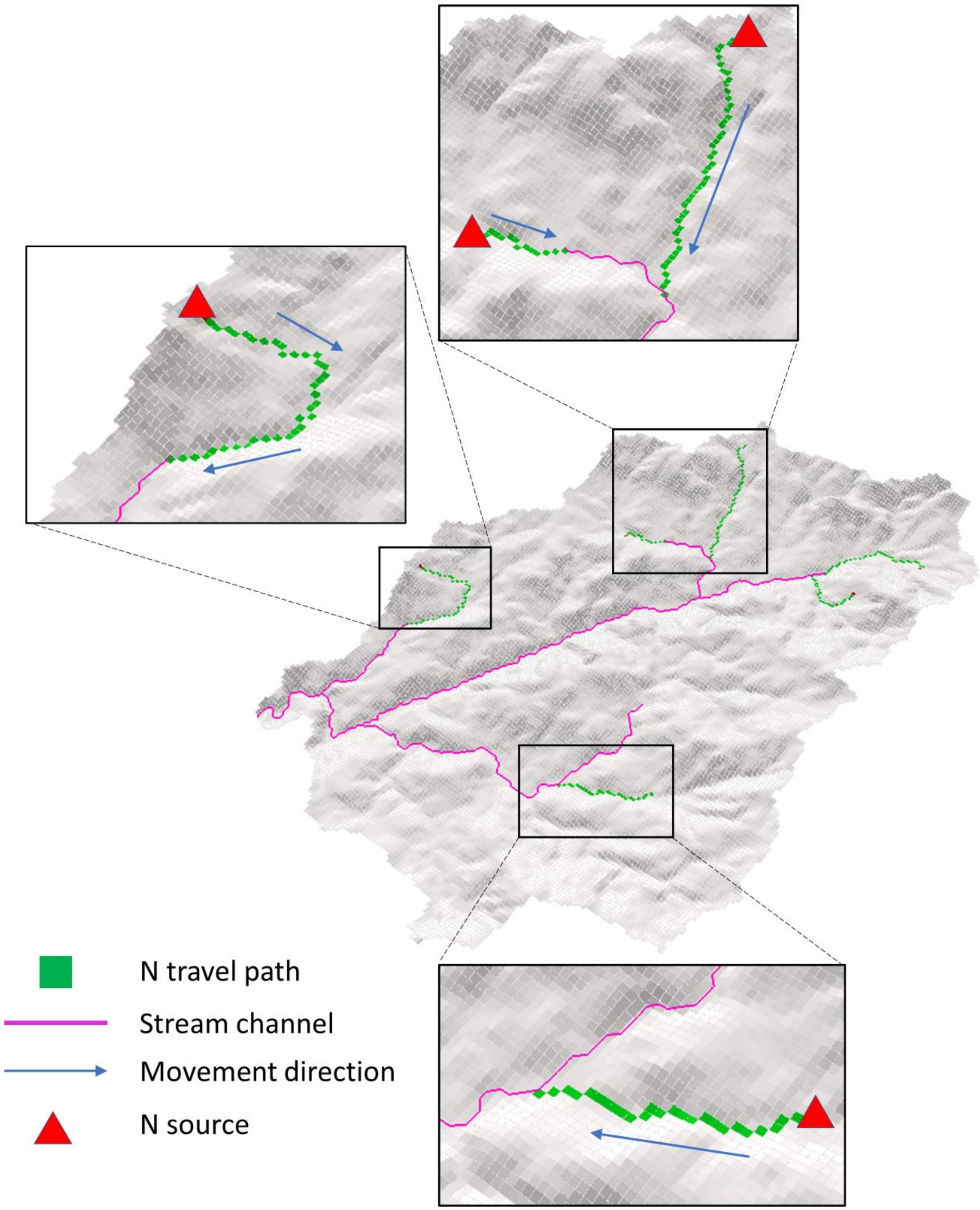

Figure 7. An example of DHSVM-N modeled nitrate pollutant overland travel path following a storm event.

Table 1. Main differences in representing relevant hydrological processes between DHSVM and SWAT.

	DHSVM	SWAT
Spatial Discretization	Watershed is divided into grids of equal size connected via flow path based on DEM.	Watershed is divided into HRUs based on vegetation type, soil type and slope. HRUs are spatially discontinuous and not allowed to interact with each other.
Modeling Unit	Regular grid cell at spatial scale of DEM data.	Irregular-shape hydrological response units (normally much larger than DHSVM's grid cell in size).
Evapotranspiration	Use two-layer canopy model.	Has the option of Penman-Monteith, Priestly-Taylor, and Hargreaves methods.
Surface Runoff	Represent both saturation and infiltration excess runoff based on groundwater table variation and the difference between soil infiltration rate and precipitation rate for each modeling grid cell.	Use SCS curve number method or Green-Ampt infiltration method.
Re-infiltration	Consider re-infiltration process.	Re-infiltration is not simulated due to no interaction between HRUs.
Flow Routing	Represent both surface and subsurface flow routing based on landscape terrain and topography. Also include channel flow routing. Use kinematic wave method for flow routing with different roughness for overland flow and channel flow. The overland flow path network and channel network used for routing are based on realistic network determined by fine-resolution DEM data.	Use modified rational method. Runoff is lagged to stream channel from individual HRU in large basins. Lateral subsurface flow is simulated by a kinematic storage model and groundwater is simulated using empirical equations. Channel routing is based on variable storage routing method or Muskingum routing method.
Snow Process	Use a comprehensive two-layer snowpack model.	Snowpack is modeled at ground surface.
Soil Moisture Movement within Soil Column	Described by Darcy's law.	Percolation is calculated by a storage routing method.
Energy and Water Budgets	Solve both energy and water balance equations.	Use a temperature-based method for snow melt.

Table 2. Mass balance of nitrogen process from simulations achieved by all three models under low/high nitrate loading condition for year 2008 – 2010. Change in percentage compared to DHSVM-N's result is marked by parenthesis.

Nitrate Flux	Low nitrate loading scenario			High nitrate loading scenario		
	SWAT	DHSVM-N	DHSVM-N_alt	SWAT	DHSVM-N	DHSVM-N_alt
Nitrate in Rainfall, kg/ha/yr	15.6	15.6	15.6	15.6	15.6	15.6
Additional Nitrate, kg/ha/yr	0.0	0.0	0.0	82.3	82.3	82.3
Nitrate from Decomposition & Mineralization, kg/ha/yr	8.6	17.2	17 (-1.2%)	16.9	22.7	22.6 (-0.4%)
Nitrate Uptake by Plant, kg/ha/yr	14.5	18.7	18.3 (-2.1%)	31.7	18.2	18.1 (-0.5%)
Nitrate Removed by Denitrification, kg/ha/yr	1.6	11.3	10.9 (-3.5%)	31.2	94.5	89.4 (+5.4%)
Nitrate Stream Export, kg/ha/yr	2.5	2.0	2.6 (+30.0%)	15.8	7.6	12.6 (+65.8%)

Table 3. Comparison of the three models regarding hydrological simulation and nitrate transport

	DHSVM-N	SWAT	DHSVM-N_alt
Feature Summary	Features include two physically based surface runoff generation mechanisms, re-infiltration process, separated routing processes for overland flow, channel flow, and subsurface flow. Grid by grid water and nitrate transport process following water flow pathways determined by topography at a high spatial resolution.	Hydrological processes are calculated based on empirical methods such as the CN method. Also, no re-infiltration process is considered. Each HRU transports water and nitrate to stream channels directly without any overland flow routing. That is, there are no interactions among different HRUs during the water and nitrate flow routing since water and nitrate are independently moved to the outlet of the watershed from each HRU.	The hydrological processes are the same as those included in DHSVM-N. Its nitrate transport processes is the same as those in SWAT except that the water and nitrate are originated from each DHSVM-N modeling grid instead of from each SWAT's HRU.

Table 4. Summary of impacts of the top 1% denitrification contribution grids and their potential maximum impact on stream nitrate export. The top 1% locations are identified as the grids in DHSVM-N whose corresponding denitrification amount is within the highest top 1%. **N**ote: the maximum stream nitrate export increase here is expressed as a ratio of the amount of the denitrification at the hot spots to the stream nitrate export. That is, it is the percentage as if the amount of nitrate at those hot spots were not consumed by denitrification but rather were all exported to strea**ms**

Locations with high denitrification capability in DHSVM-N	Low nitrate loading scenario			High nitrate loading scenario		
	SWAT	DHSVM-N	DHSVM-N_alt	SWAT	DHSVM-N	DHSVM-N_alt
Denitrification (kg N/ha/yr)	0.02	0.4	0.1	0.4	2.9	0.6
Denitrification Contribution (%)	1.5	3.7	1.3	1.4	3.1	0.7
Stream Nitrate Export (kg N/ha/yr)	2.5	2	2.6	15.8	7.6	12.6
Maximum Stream Nitrate Export Increase (%)	0.8	20.0	3.8	2.5	38.2	4.8